Quarterly Progress Report

For Period

April 1 to June 30, 1967

FUNDAMENTAL STUDIES OF THE METALLURGICAL, ELECTRICAL, AND OPTICAL PROPERTIES OF GALLIUM PHOSPHIDE

Grant No. NsG-555

Prepared For

NATIONAL AERONAUTICS AND SPACE ADMINISTRATION
LEWIS RESEARCH CENTER
CLEVELAND, OHIO

Work Performed By

Solid-State Electronics Laboratories
Stanford University
Stanford, California

second. The temperature was measured by a chromel-alumel thermocouple which was attached to the transistor header on which the sample was mounted. The photocurrent versus temperature was recorded on an x-y recorder. The voltage across the sample was 67.5 v. The following filters were used: neutral filters, germanium, gallium arsenide and interference filter No. 500 of set No. 3112 made by Optics Technology, Inc. This last filter has a transmission range of $4800\text{Å} < \lambda < 5200\text{Å}$ which indicates the energy corresponding to the band gap of GaP. The photocurrent did not depend on the voltage polarity and changed in the same way during cooling or heating cycles.

2. Results and Discussion

The spectral photoresponse per incident photon for four samples of GaP:Co are presented in Figs. 1a - 1d. The highest amount of cobalt was introduced into samples C3 and C2 and the smallest into sample C6 (see Table I). An increase of cobalt concentration reduced the photoconductivity around the band edge thus indicating that higher numbers of unfilled cobalt acceptors reduce the lifetime of electrons. The peak at 0.7 μ can be attributed to transitions from filled acceptor levels to the conduction band. This is in agreement with the energy of filled cobalt levels.[1] This peak is reduced in the same ratio as the peak connected with band-to-band photoconductivity when the amount of cobalt is increased. Therefore, the suggestion that it is connected with transitions from filled cobalt levels to the conduction band is valid. The long tail of photoconductivity at wavelengths greater than 2 μ is more pronounced in the samples with a larger amount of cobalt;

PROJECT 5109: PHOTOCONDUCTIVITY OF GaP DOPED WITH COBALT, IRON AND TITANIUM

National Aeronautics and Space Administration
Grant NsG-555
Project Leader: G. L. Pearson
Staff: J. Baranowski

In the last quarter we reported the preliminary results for photoconductivity of GaP with unfilled cobalt and iron levels. In this quarter we continued this study using more accurate experimental techniques.

1. Experiment

Seven samples of GaP were prepared and measured, four doped with cobalt, one doped with iron, one doped with titanium and one doped with cobalt and zinc. The carrier concentration, mobility and diffusion parameters are presented in Table I. Metals used as a dopant were evaporated on both sides of the sample prior to diffusion. After diffusion the same samples were lapped on both sides then mechanically and chemically polished. The chemical etch was made of 2 parts HCl and 1 part HNO_3. Contacts were applied at either end of rod-type samples by alloying evaporated layers of 98% gold - 2% zinc at 500°C in forming gas. Spectral distribution of the photoresponse was measured in a Cary Model 14IR Spectrophotometer by an a.c. method at a frequency of 30 cycles per second. The source was calibrated by a thermopile. A PbS cell was used as a reference for a PAR lock-in amplifier. The voltage across the sample was 67.5 v. All measurements of spectral distribution were taken at room temperature.

The temperature dependence of photocurrent was measured by an a.c. method using a frequency of light modulation of 600 cycles per

therefore, it is probably connected with transitions from the valence band to unfilled acceptor levels. Because of the small signal, we were not able to extend these measurements to longer wavelengths; thus we are not able to draw any definite quantitative conclusions such as the position of the unfilled acceptor levels or the energies at the maxima of the valence band density of states.

The results for GaP doped with iron and titanium are presented in Figs. 2 and 3. The spectral behavior of photoconductivity is similar to that for GaP:Co. For the same reasons as stated above, we can draw no quantitative conclusions.

Gallium phosphide doped with cobalt, iron and titanium showed interesting effects of a decrease in photocurrent when the temperature was lowered. The dependence of photocurrent on temperature for GaP:Co is shown in Figs. 4a-4c. The most drastic changes of photocurrent occurred when the sample was illuminated with light of energy corresponding to the energy gap. This suggests that two different mechanisms for recombination are present in this range of temperature. The slopes of the increase of photocurrent under illumination of light at $\lambda = 5000\text{Å}$ as a function of 1/T are given in Table II, together with the slopes of dark current. It is interesting to note that for some samples the slopes of photocurrent are greater than the ones of dark current. The sum of these two slopes is approximately constant. This suggests that excited states of the acceptor level can play an important role in the recombination and trapping processes. Because we do not know the nature of the acceptor level it is difficult to discuss the excited states. As J. W. Allen[2] points out, the unfilled acceptor

levels of the transition metals are very often neither of d^{n-1} configuration nor hydrogenic. The wavefunction of such a center is probably a mixture of d^{n-1} configuration and a hole in the bonding orbitals. Without detailed calculations similar to those of J. L. Birman[3] for copper in ZnS, it is impossible to present a good model for this type of center in GaP.

Data for GaP:Fe and GaP:Ti are similar to those obtained for GaP:Co. These results are presented in Fig. 5 and Figs. 6a - 6b respectively. These results indicate that the same mechanism for photoconductivity is responsible for the strange behavior of photocurrent with changes in temperature for GaP:Co, Ga:Fe, and Ga:Ti. We do not give an explanation here for this effect because the model must be based on a knowledge of the nature of the unfilled acceptor levels. As pointed out above, we lack sufficient information to thoroughly understand the mechanism.

REFERENCES

1. D. H. Loescher, J. W. Allen and G. L. Pearson, Proc. Int. Conf. Physics of Semiconductors, Kyoto, Japan (1966), p. 239.

2. J. W. Allen private communication.

3. J. L. Birman, Luminescence Conference, Budapest, Hungary (invited paper) August 1965.

FIGURE CAPTIONS

Fig. 1 Spectral photoresponse per incident photon

a) For Sample C2
b) For Sample C3
c) For Sample C4
d) For Sample C6

Fig. 2 Spectral photoresponse per incident photon for Sample I2.

Fig. 3 Spectral photoresponse per incident photon for Sample T1 and Sample T2.

Fig. 4 Dependence of photocurrent on temperature

a) For Sample C2
b) For Sample C3
c) For Sample C4
d) For Sample C6
e) For Sample C1Z

Fig. 5 Dependence of photocurrent on temperature for Sample I2.

Fig. 6a Dependence of photocurrent on temperature for Sample T2.

Fig. 6b Dependence of photocurrent on temperature for Sample T2.

Sample	Concentration before diff. (cm^{-1})	Mobility cm^2/v-sec	Dopant	Temp. of the diff.	Time of the diff.
C2	5×10^{15}	120	Co	1280°C	24 hrs
C3	6×10^{15}	105	Co	1320°C	18 hrs
C4	6×10^{15}	105	Co	1200°C	24 hrs
C6	6×10^{15}	105	Co	1100°C	8 hrs
I2	5×10^{15}	120	Fe	1180°C	20 hrs
T2	6×10^{15}	105	Ti	1300°C	18 hrs
T1	6×10^{15}	105	Ti	1300°C	18 hrs
C1Z	6×10^{15}	105	1) Co	1300°C	24 hrs
			2) Zn	800°C	2 hrs
			3) Annealing	1160°C	12 hrs

TABLE I - The Parameters of the Materials Before Diffusion and Conditions of the Diffusions.

Sample	Slope of the dark current	Slope of the photocurrent (light $\lambda \approx 5000\text{Å}$)	Sum of two slopes
C2	0.30 eV	0.25 eV	0.55 eV
C3	0.25 eV	0.34 eV	0.59 eV
C4	0.26 eV	0.31 eV	0.58 eV
C6	0.37 eV	0.24 eV	0.61 eV
C1Z	0.17 eV	0.13 eV	0.30 eV
I2	0.29 eV	0.21 eV	0.50 eV
T2	0.38 eV	0.34 eV	0.72 eV

TABLE II - The Slopes of the Dark Current and Photocurrent

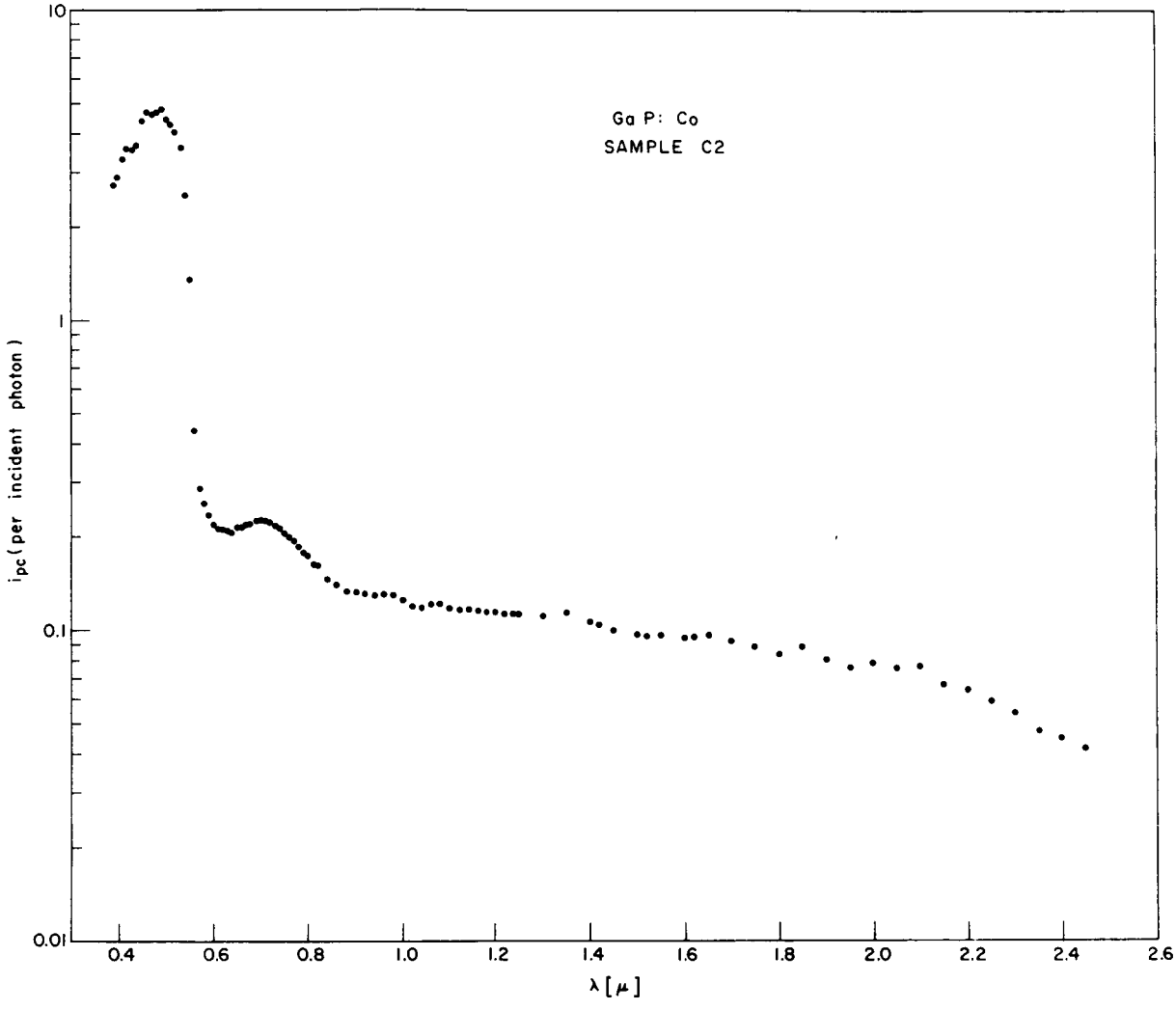
Ga P: Co
SAMPLE C2
10
1
0.1
0.01
i_{pc} (per incident photon)
0.4
0.6
0.8
1.0
1.2
1.4
1.6
1.8
2.0
2.2
2.4
2.6
λ [μ]

Fig. 1a

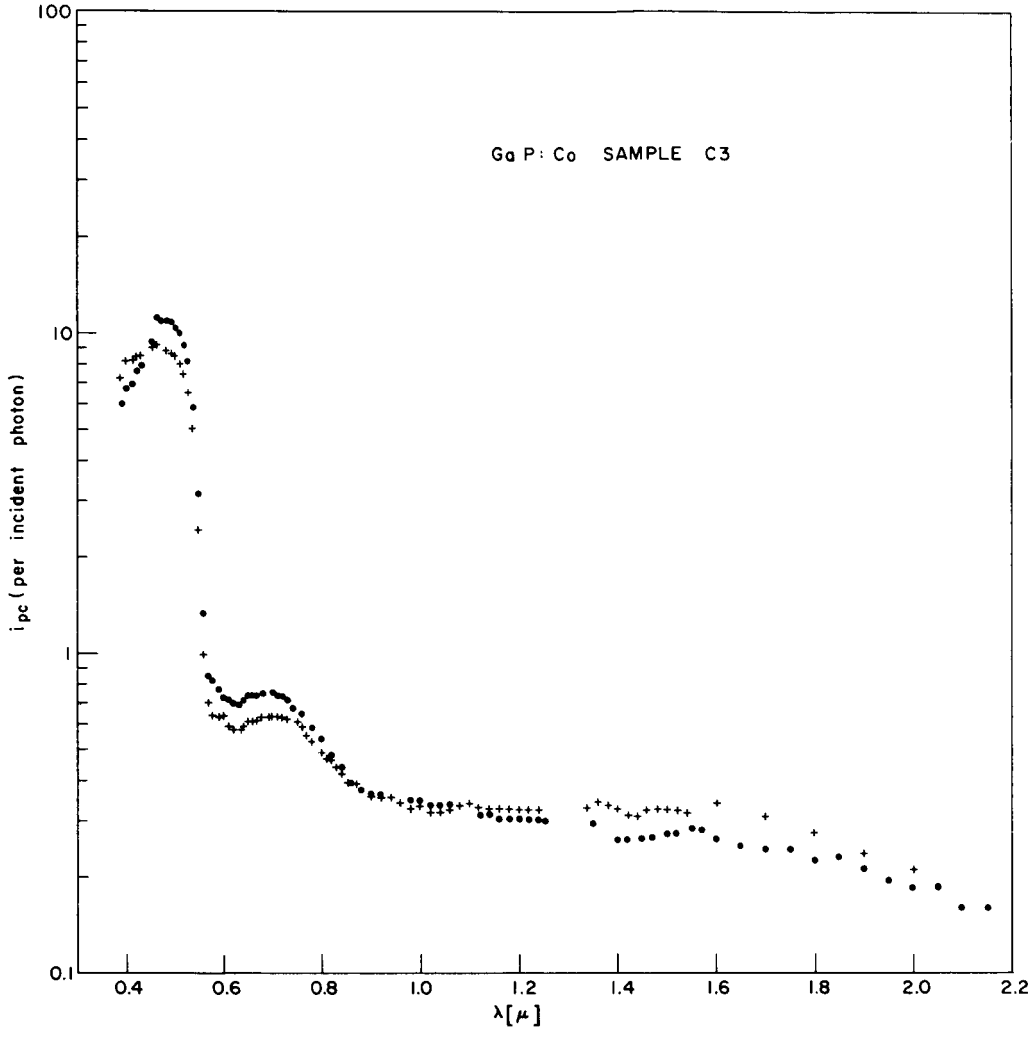
Ga P: Co SAMPLE C3
100
10
1
0.1
i_{pc} (per incident photon)
0.4
0.6
0.8
1.0
1.2
1.4
1.6
1.8
2.0
2.2
λ[μ]

Fig. 1b

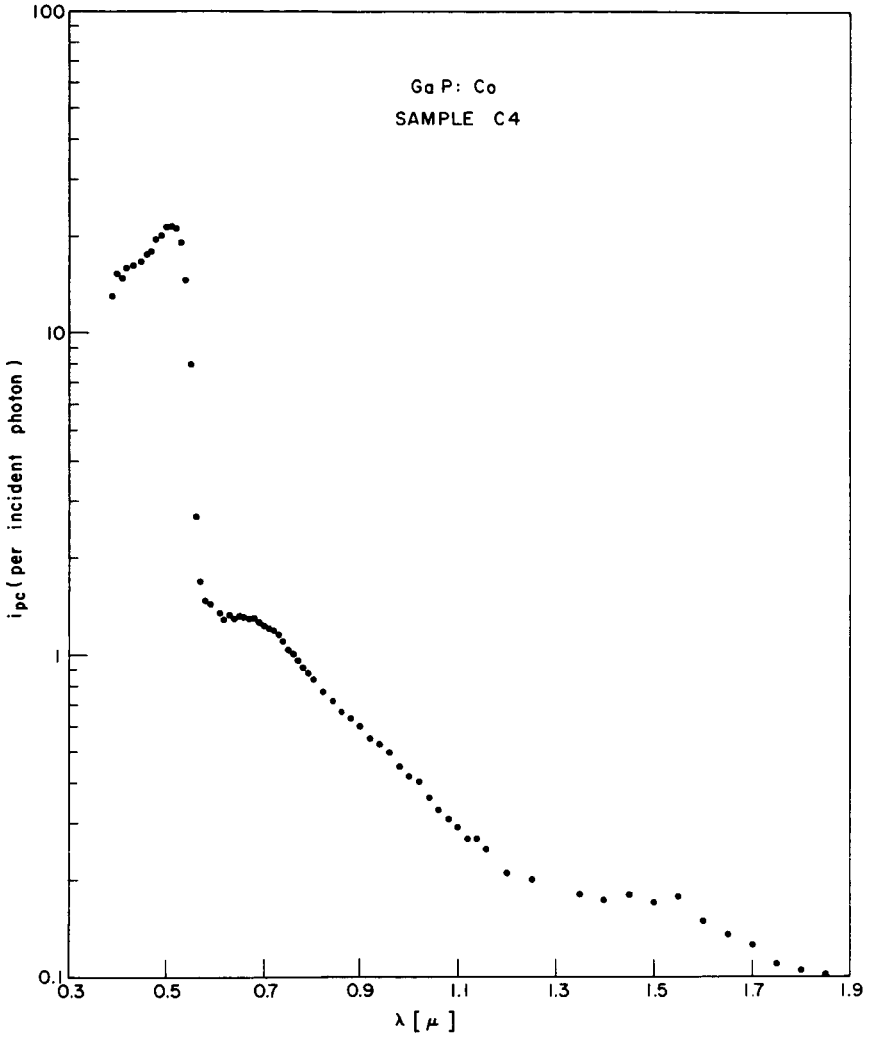
Ga P: Co
SAMPLE C4
100
10
1
0.1
i_{pc} (per incident photon)
0.3
0.5
0.7
0.9
1.1
1.3
1.5
1.7
1.9
λ [μ]

Fig. 1c

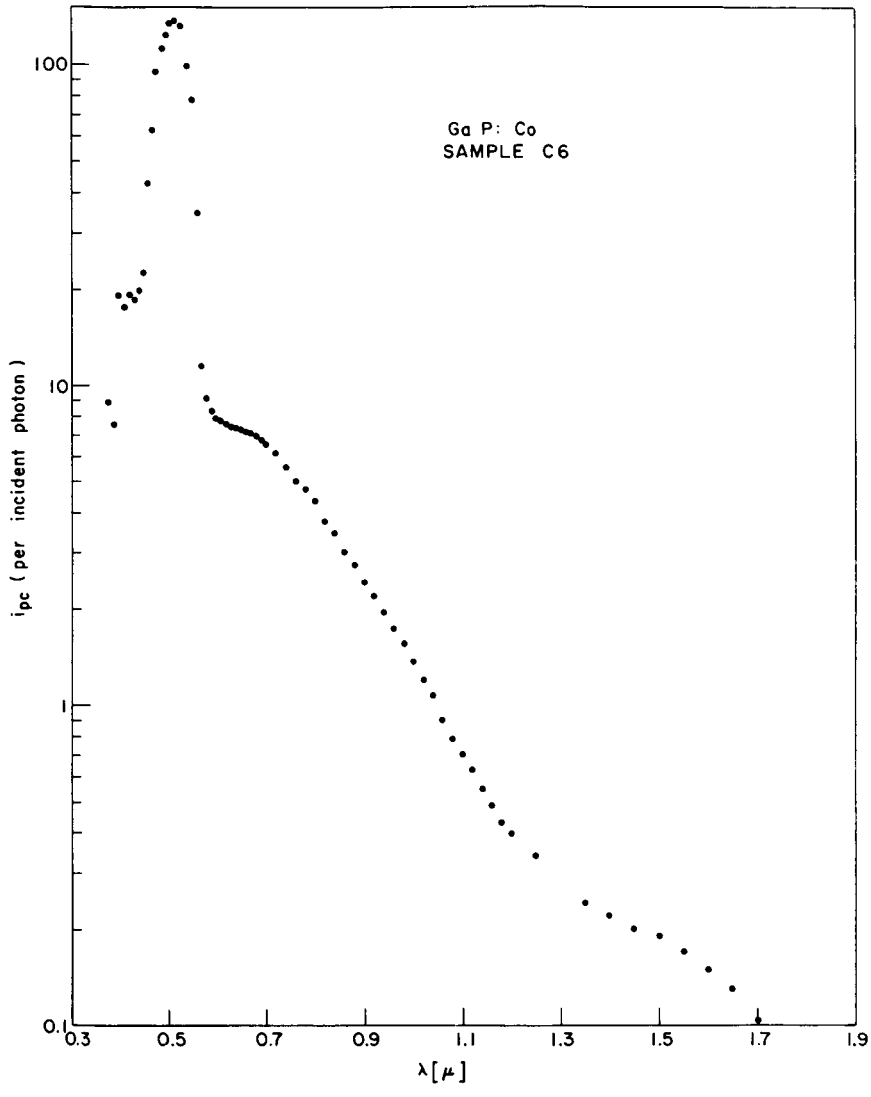
Ga P: Co
SAMPLE C6
100
10
1
0.1
i_{pc} (per incident photon)
0.3
0.5
0.7
0.9
1.1
1.3
1.5
1.7
1.9
λ[μ]

Fig. 1d

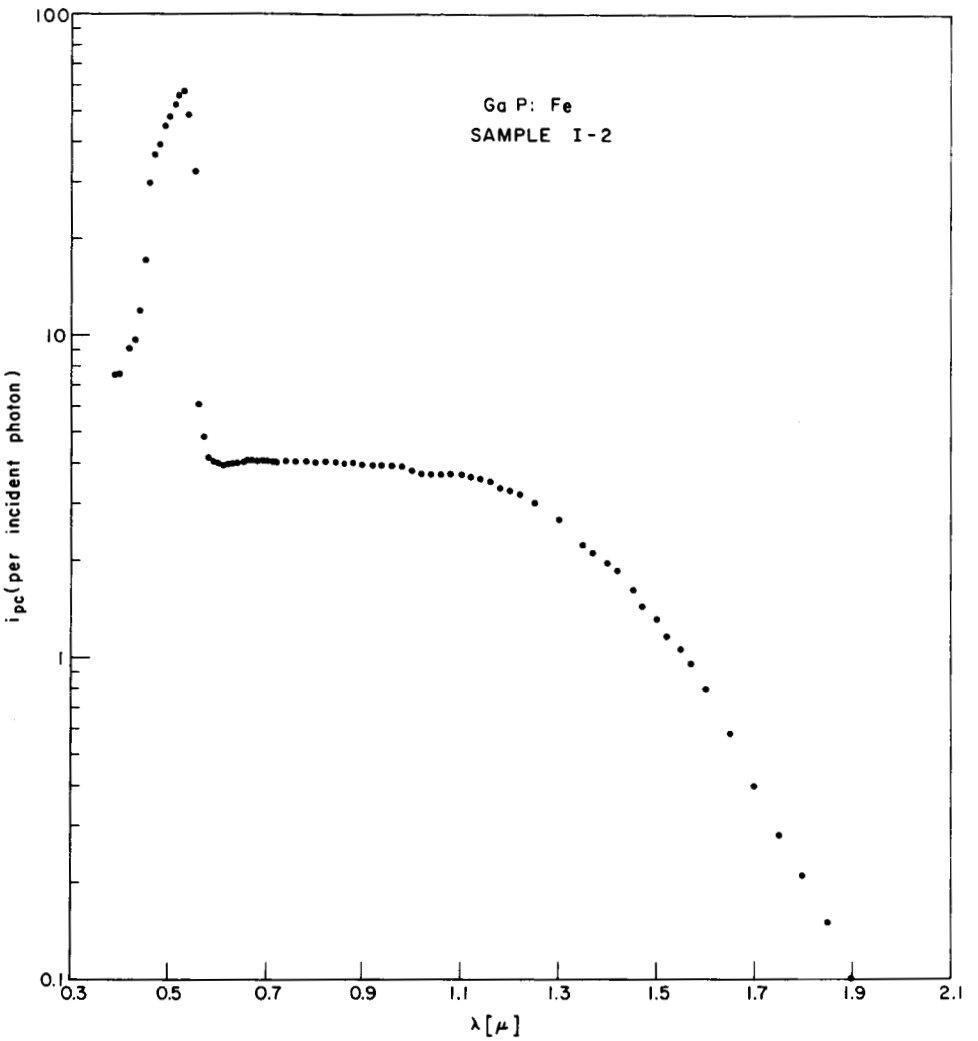
Ga P: Fe
SAMPLE I-2
100
10
1
0.1
i_{pc} (per incident photon)
0.3
0.5
0.7
0.9
1.1
1.3
1.5
1.7
1.9
2.1
λ[μ]

Fig. 2

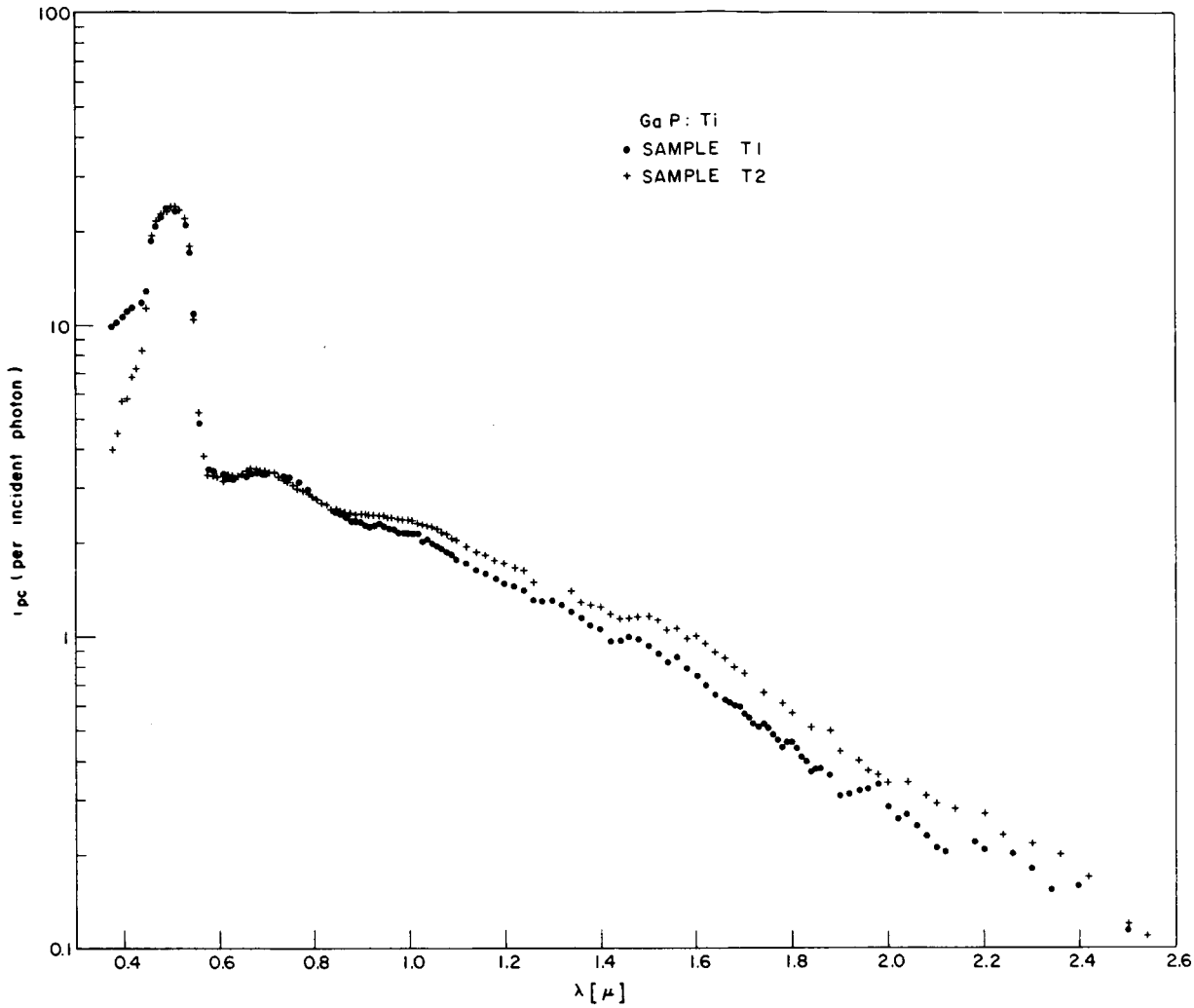
Ga P : Ti
• SAMPLE T1
+ SAMPLE T2
100
10
1
0.1
Ipc (per incident photon)
0.4
0.6
0.8
1.0
1.2
1.4
1.6
1.8
2.0
2.2
2.4
2.6
λ [μ]

Fig. 3

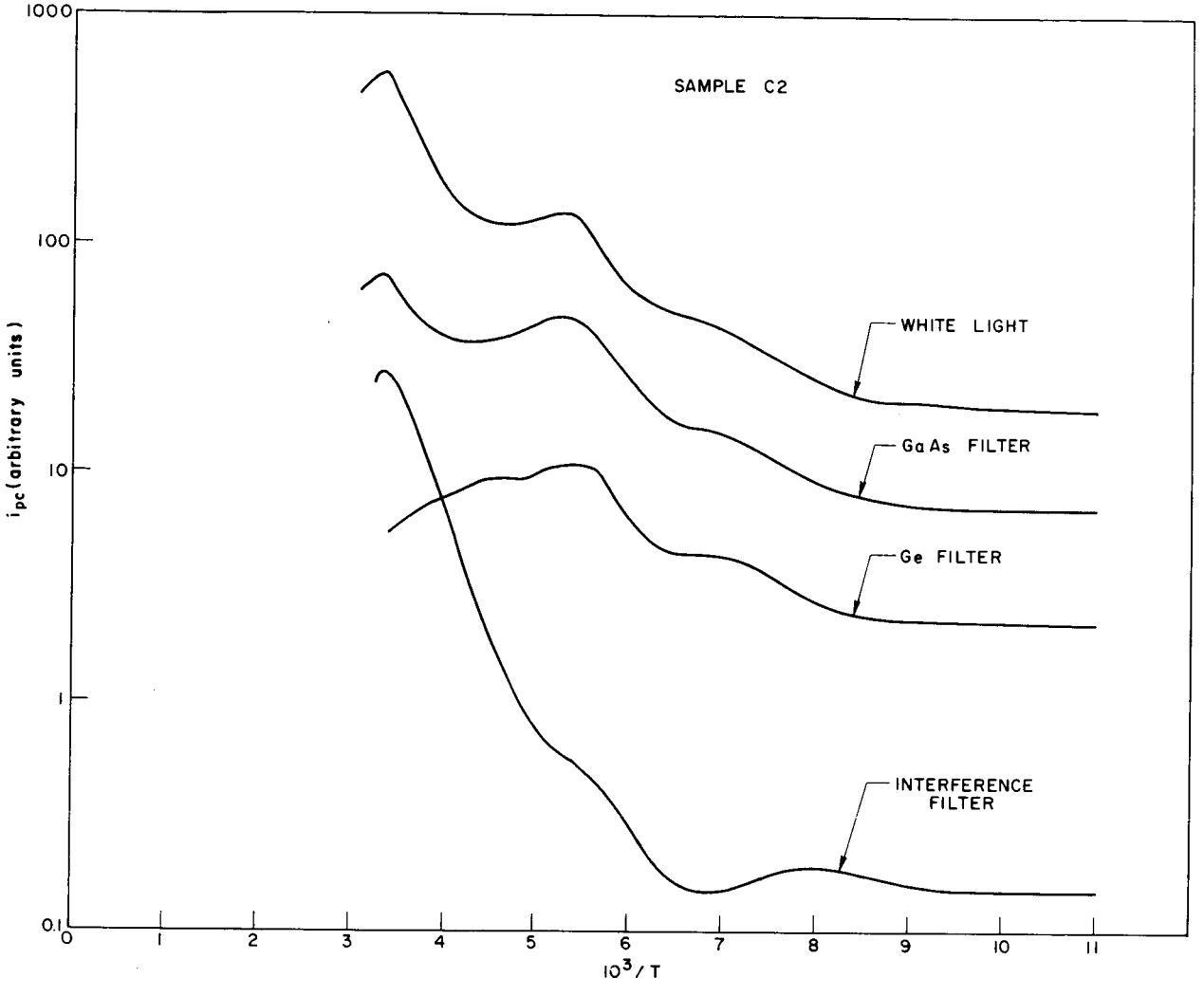
SAMPLE C2
WHITE LIGHT
GaAs FILTER
Ge FILTER
INTERFERENCE FILTER
1000
100
10
1
0.1
i_{pc} (arbitrary units)
0
1
2
3
4
5
6
7
8
9
10
11
$10^3/T$

Fig. 4a

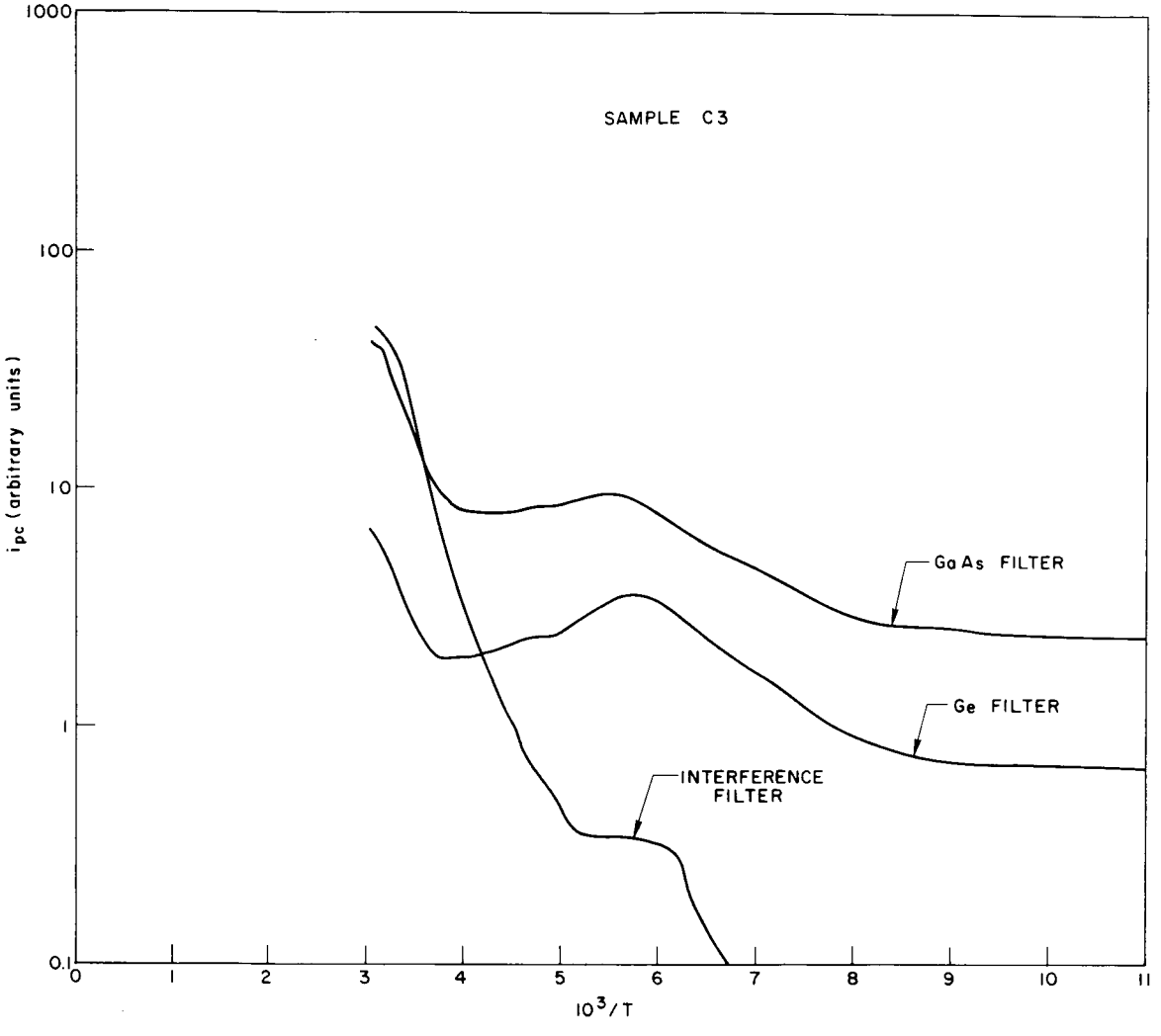
SAMPLE C3
1000
100
10
1
0.1
i_{pc} (arbitrary units)
GaAs FILTER
Ge FILTER
INTERFERENCE FILTER
0
1
2
3
4
5
6
7
8
9
10
11
$10^3/T$

Fig. 4b

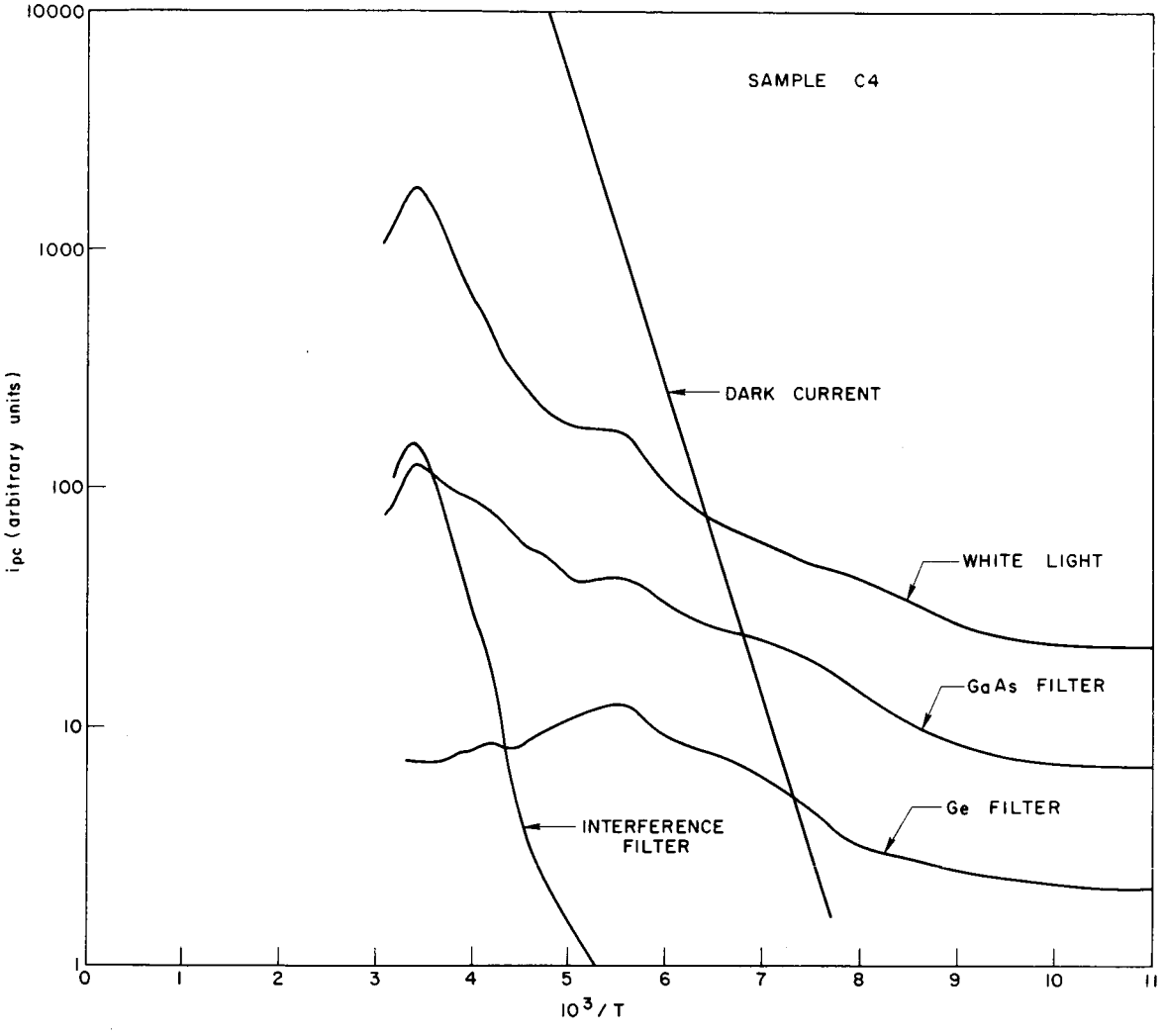
SAMPLE C4
DARK CURRENT
WHITE LIGHT
GaAs FILTER
Ge FILTER
INTERFERENCE FILTER
10000
1000
100
10
1
i_{pc} (arbitrary units)
0
1
2
3
4
5
6
7
8
9
10
11
$10^3/T$

Fig. 4c

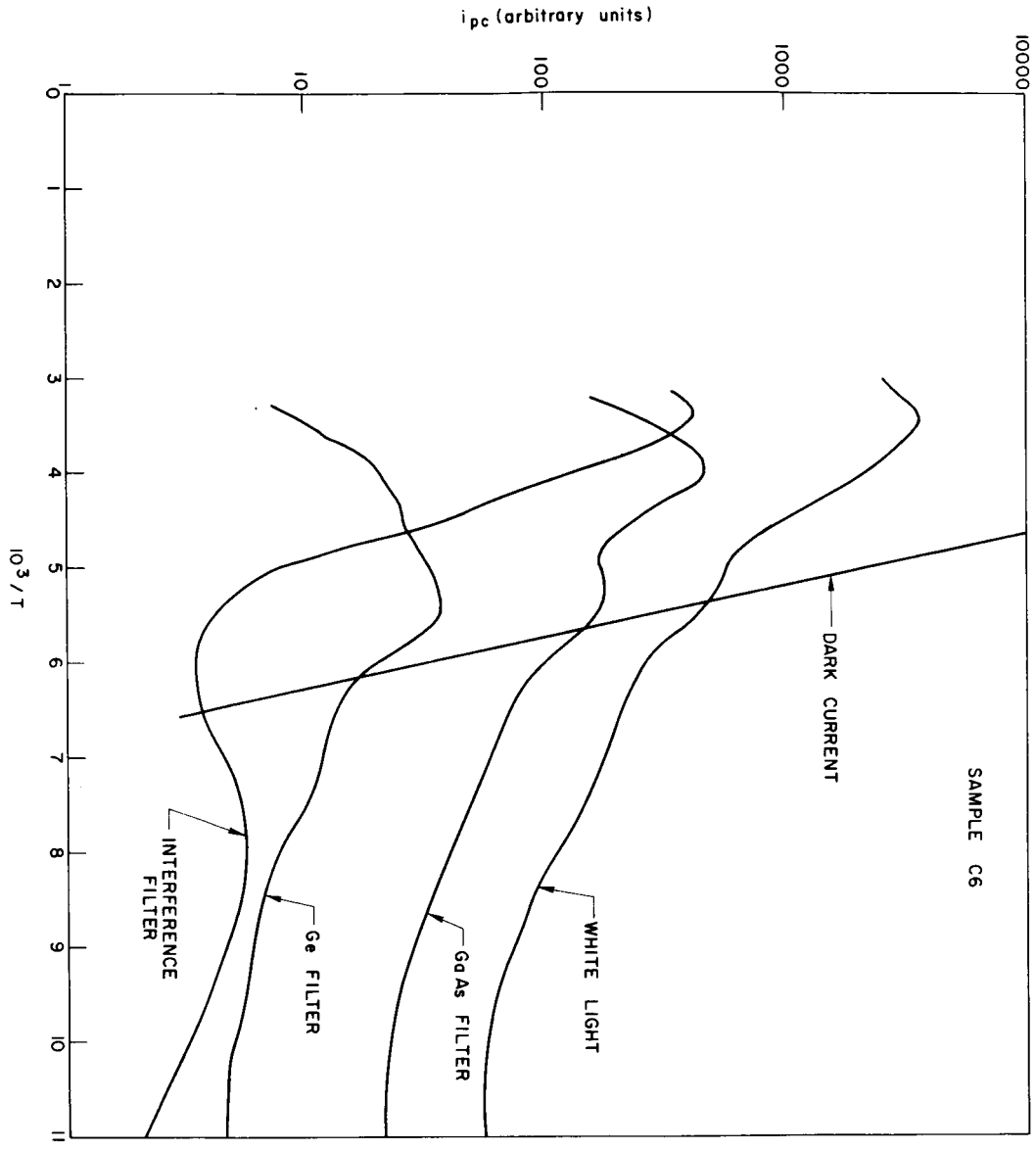
i_{pc} (arbitrary units)
1
10
100
1000
10000
0
1
2
3
4
5
6
7
8
9
10
11
$10^3/T$
SAMPLE C6
DARK CURRENT
WHITE LIGHT
GaAs FILTER
Ge FILTER
INTERFERENCE FILTER

Fig. 4d

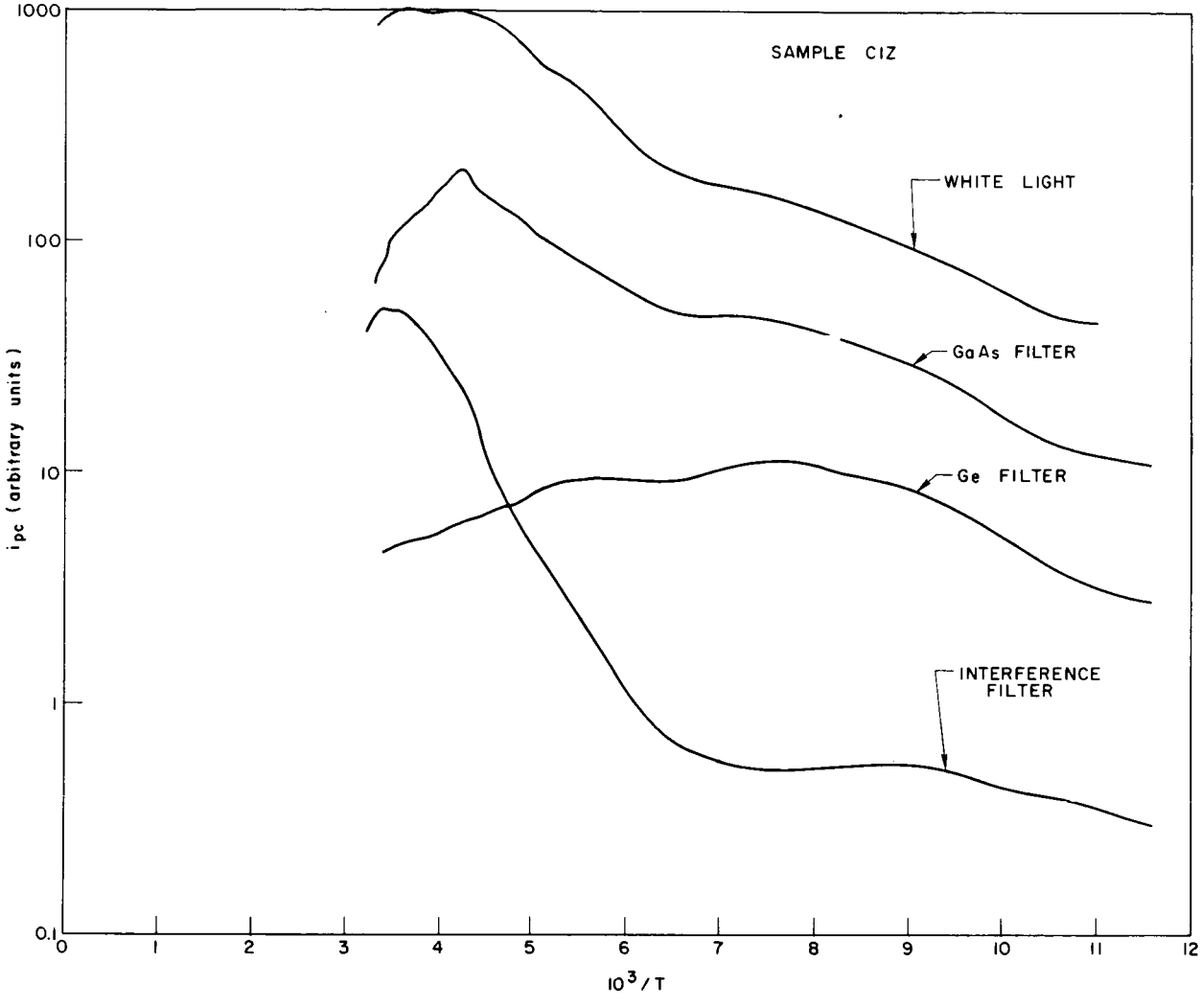
SAMPLE CIZ
WHITE LIGHT
GaAs FILTER
Ge FILTER
INTERFERENCE FILTER
1000
100
10
1
0.1
i_{pc} (arbitrary units)
0
1
2
3
4
5
6
7
8
9
10
11
12
$10^3/T$

Fig. 4e

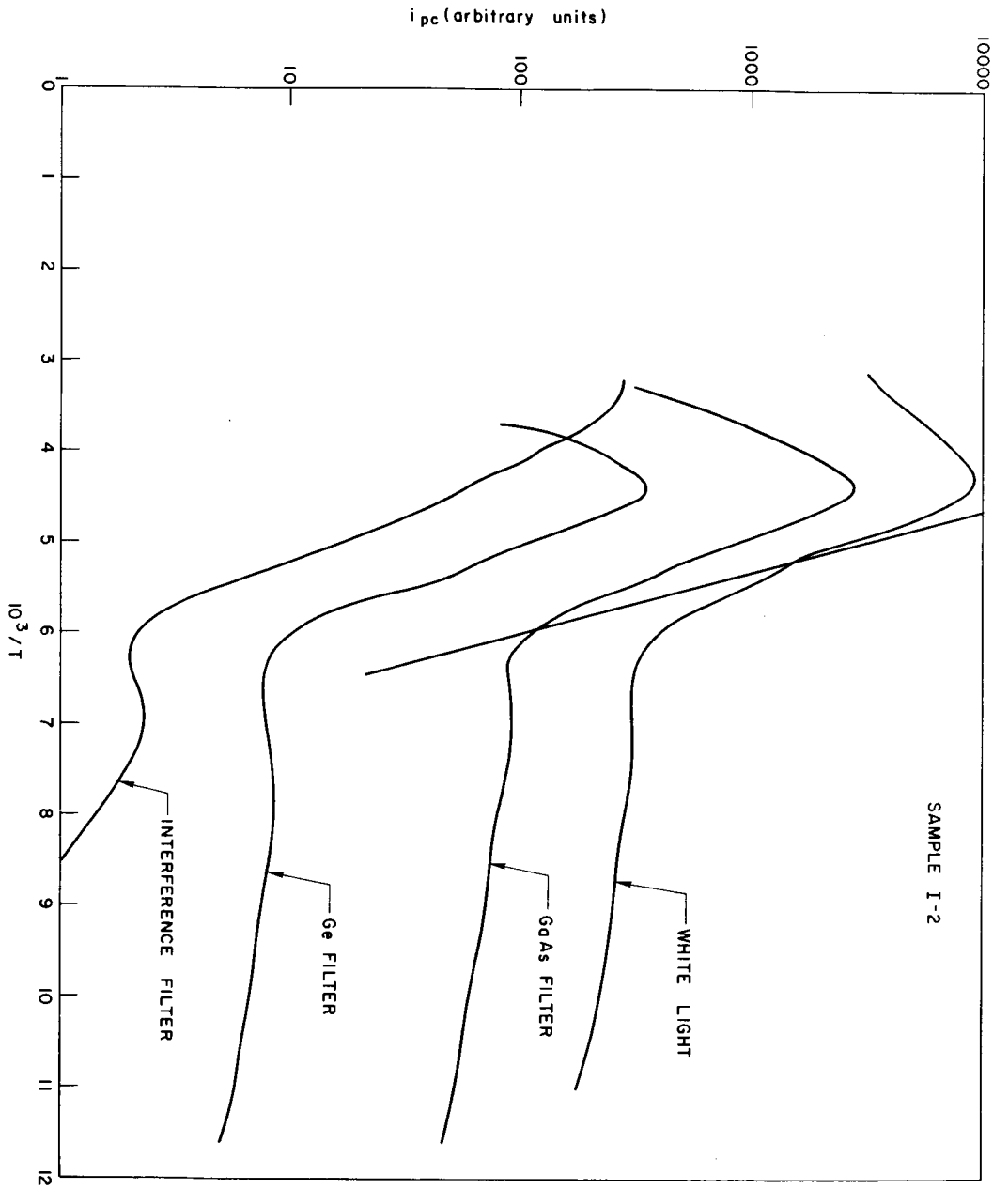
i_{pc} (arbitrary units)
1
10
100
1000
10000
0
1
2
3
4
5
6
7
8
9
10
11
12
$10^3/T$
SAMPLE I-2
WHITE LIGHT
GaAs FILTER
Ge FILTER
INTERFERENCE FILTER

Fig. 5

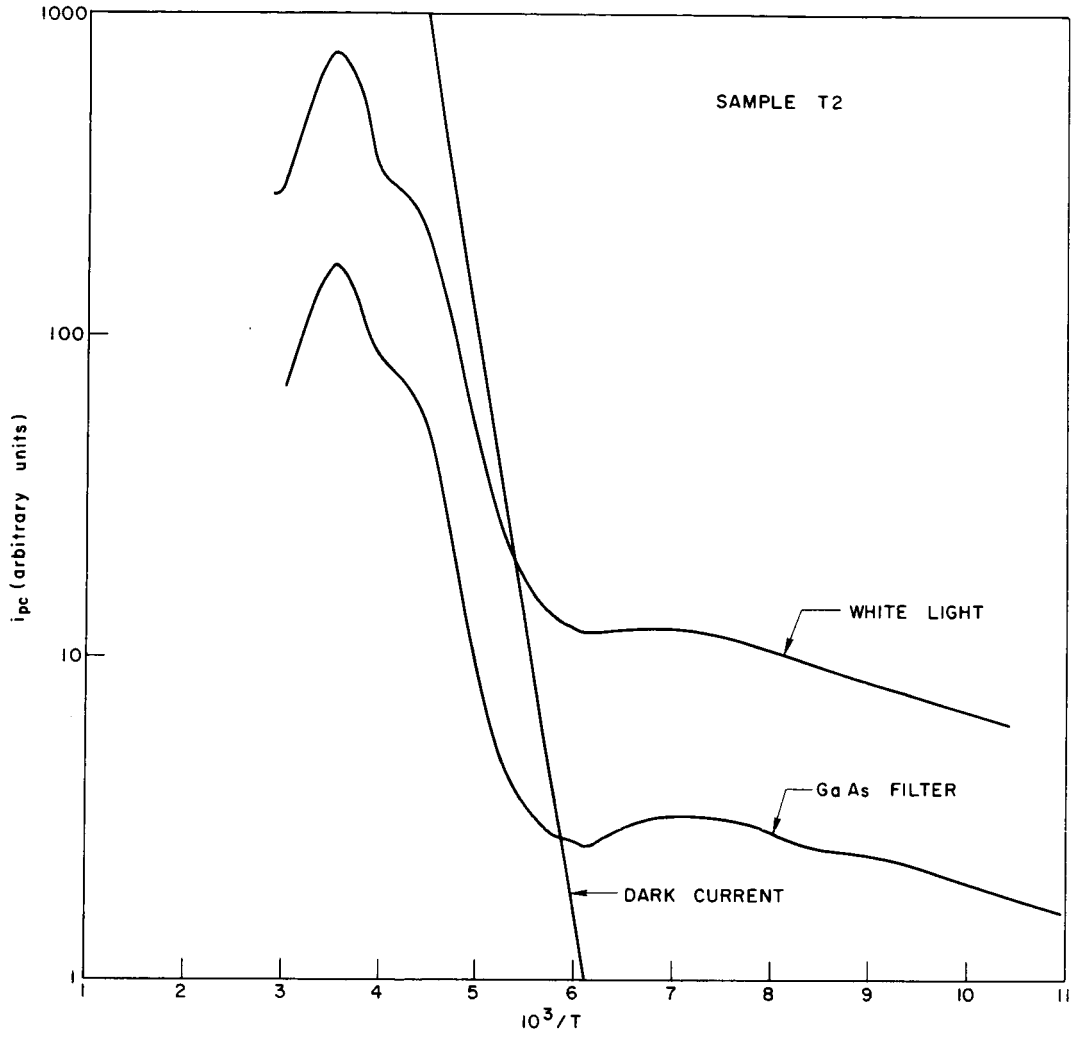
SAMPLE T2
WHITE LIGHT
Ga As FILTER
DARK CURRENT
1000
100
10
1
i_{pc} (arbitrary units)
1
2
3
4
5
6
7
8
9
10
11
$10^3/T$

Fig. 6a

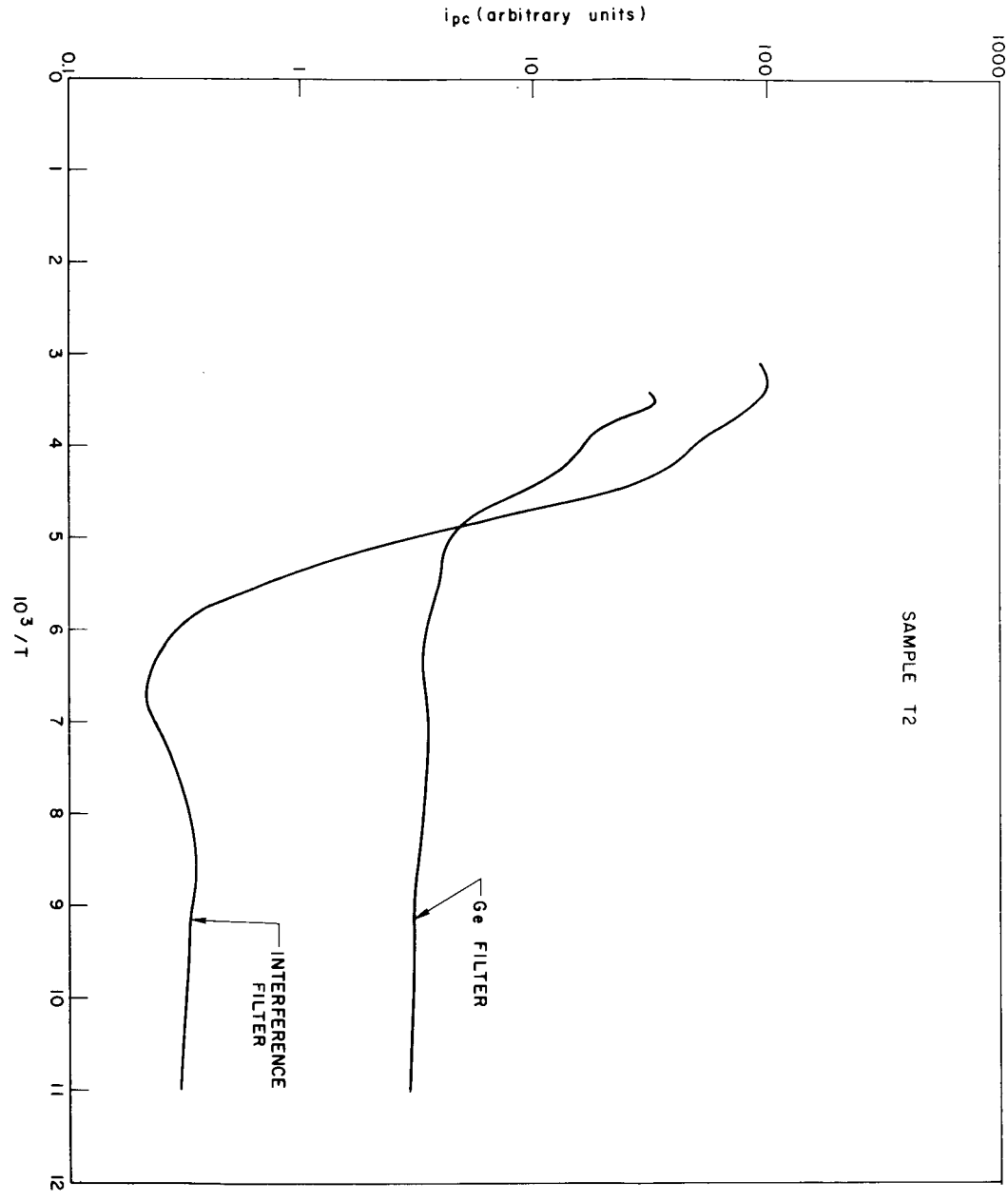
i_{pc} (arbitrary units)
0.1
1
10
100
1000
0
1
2
3
4
5
6
7
8
9
10
11
12
$10^3/T$
SAMPLE T2
Ge FILTER
INTERFERENCE FILTER

Fig. 6b

PROJECT 5112: THE PROPERTIES OF RECTIFYING JUNCTIONS IN $GaAs_xP_{1-x}$

National Aeronautics and Space Administration
Grant NsG-555
Project Leader: G. L. Pearson
Staff: S. F. Nygren*

The purpose of this project is to study the preparation and characterization of rectifying junctions in GaP and $GaAs_xP_{1-x}$. In particular, we wish to relate the structure of the crystals to the electrical properties of the junctions. During this quarter, we have grown several GaP single crystals by vapor epitaxy. We have studied zinc diffusion spikes in GaP as a function of temperature, and we have begun to make p-n junctions in GaP by the liquid phase epitaxial technique.

A. Crystal Growth

Four undoped and four sulfur doped GaP crystals were grown by vapor epitaxy. All eight crystals were n-type and ohmic contacts could be made to them by alloying tin dots to the GaP. Room temperature electrical measurements were made using the Van der Pauw technique. Carrier concentrations vs. mobilities are plotted in Fig. 1. For comparison, data from 34 other crystals grown in this laboratory are also included in Fig. 1. It may be seen that undoped and lightly doped crystals are of widely varying quality, having mobilities that range from 60 to 155 cm^2/v sec. On the other hand, the more heavily doped crystals ($n > 4 \times 10^{17}$ cm^{-3}) have mobilities that may be related to carrier concentrations in a predictable way.

---

*NSF Fellow

B. Diffusion Spikes

Our study of the irregular diffusion front of zinc in GaP in the presence of crystal defects has been continued. During this quarter we have investigated the relationship between the depth of the diffusion spikes and the diffusion temperature. Five diffusions were performed at different temperatures; they are summarized in Table 1. The diffusion ampoules were 0.2 cm^3 quartz tubes evacuated to 4×10^{-5} mm Hg. The GaP samples were all cut from the same (111) oriented crystal; they measured about $3.0 \times 2.5 \times 0.39$ mm^3, and their surfaces were mechanically polished. The diffusion source was a powder of 75% GaP - 25% Zn, chosen to help minimize the attack on the surfaces of the GaP samples. The source was preannealed in an evacuated ampoule at $1014^{\circ}C$ for 23 hours. All diffusions were terminated by quenching the ampoules in ice water.

The results of the diffusions were examined by cross-sectioning the crystals on {111}Ga planes that were inclined to the sample surfaces and then etching the samples in the {111}Ga etchant. In this way the diffusion front and the crystal defects were revealed. A double diffusion front was seen in the samples that were diffused at the three highest temperatures. The diffusion spikes were found to correlate well, but not exactly, with etch lines corresponding to crystal faults.

The measured junction depth is normalized to a diffusion time of one hour and is plotted in Fig. 2. The normalization is done by assuming that our diffusions were done at a high enough

temperature and for a long enough time that the junction depth, x_j, is given by

$$x_j = A \sqrt{t}\ e^{-B/kT}$$

where t = time, A, B are constants and T = absolute temperature. L. Chang[1] gives evidence that this formula is valid for $800^{\circ}C < T < 1000^{\circ}C$. Actually, recent experiments by C. H. Ting[2] suggest that the relationship should be

$$x_j = A\ [\sqrt{t} - C(T)]\ e^{-B/kT}$$

where C(T) decreases as temperature increases. We assume that we can ignore C(T). Then the three lowest temperature points define a curve in which $A = e^{15.96}$ microns/ $\sqrt{\text{time}}$, B = 1.23. This agrees well with Chang's result that $A = e^{17.0}$ microns/ $\sqrt{\text{time}}$, B = 1.35. The extension of the curve may be used to find that the effective warm-up time for a diffusion is 2.1 minutes at $907^{\circ}C$, and 3.16 minutes at $998^{\circ}C$.

The maximum spike depths are measured at points where the crystal faults extend beyond the diffusion spikes. These depths are then normalized to one hour using the effective diffusion time and are plotted in Fig. 2.

An interpretation of the diffusion spikes is not possible at this time. The exponential dependence of spike depth on reciprocal temperature suggests that the processes involved in creating diffusion spikes are thermally activated and require a lower activation energy than diffusion through the bulk. The exact mechanism and the crystal defect responsible for the diffusion spikes is not clear, however.

Queisser[3] reports that there is no enhanced diffusion of phosphorus at a coherent twin boundary in silicon, and Williams[4] reports that there is no enhanced diffusion of zinc at stacking faults in vapor epitaxial $GaAs_xP_{1-x}$. On the other hand, Kulikov and Givargizov[5] report enchanced diffusion of antimony at stacking faults in vapor epitaxial germanium layers.

C. Liquid Epitaxy

The process of growing single crystal layers on a seed crystal by liquid phase epitaxy was first reported by Nelson,[6] who used the technique with GaAs and Ge. This method has certain advantages in that it is simple; that a thin layer of the seed surface is dissolved to provide a clean and damage-free growth surface; and that p-n junctions may be formed without creating diffusion-induced defects. The technique was readily extended to GaP, and high efficiency electroluminescent diodes have been made by this method.[7]

We have begun to make p-n junctions by this technique, closely following Nelson's method. A mechanically polished, (111) oriented, n-type, vapor grown GaP substrate crystal is held down in one end of a pyrolytic graphite boat by a graphite weight. A mixture of Ga, GaP, and a dopant is placed in the other end of the boat, using enough GaP that the mixture will be saturated at the operating temperature. The boat is enclosed in a quartz tube and held in a purified hydrogen atmosphere that is flowing at 150 cm^3/min. The boat is heated to the operating temperature. Then the furnace is turned off and the boat is tipped so that the solution flows over the substrate. As the solution cools, a single crystal layer of doped

GaP is grown on the substrate. When the furnace reaches 500°C, the boat is tilted back to its original position, and the boat is moved to the cool end of the quartz tube. The gallium solution has a GaP crust, and it is still resting on top of the substrate crystal. The substrate is plucked from the Ga, and the rest of the Ga-GaP-dopant mixture is saved for reuse. The Ga that remains on the grown crystal can be removed by digestion in hot HCl or HNO_3.

In the first two runs we followed Lorenz and Pilkuhn's[8] experimental details. The source was made up of 5.0g Ga, 0.60 g GaP, and 4.0 mg Zn, an acceptor dopant in GaP. At 1140°C, 5.0 g Ga will be saturated by 0.60 g GaP. The furnace was heated to 1140°C in about 70 minutes. Then the furnace was shut off, and the initial cooling rate was about 13° c/min. Sample LEP1 had the overgrowth on the {111}P face; sample LEP3, on the {111}Ga face. The overgrowths were examined by cleaving the samples on {110} and etching the cleavage face in the {111}Ga etchant. The two overgrowths were quite similar: about 115μ of seed was removed before growth began; about 70μ of layer was grown; a second boundary was seen about 25μ from the surface of the overgrowth. (See Fig. 3 for a cross section of LEP1.) The growth surface of LEP1 was terraced slightly (see Fig. 4), and the growth surface of LEP3 was etched severely by the crystal recovery procedure. Since the net result is a {111}P surface that is smoother than the {111}Ga surface, we shall grow on {111}P surfaces in the future.

The etch patterns on a {111}Ga cross section of LEP1 suggest that the faults in the seed are inhibited from growing into the overgrowth (see Fig. 5). Also, electroluminescence and photovoltaic tests

show that the only p-n junction in LEP1 is at the seed/overgrowth interface. The surface layer is thus apparently p-type, but has a different carrier concentration so that it etches differently from the deeper layer of the overgrowth. The surface layer may be due to the segregation of an unknown impurity; the GaP source material was polycrystal of unknown origin.

Tests revealed that much of the surface layer that is removed from the seed is removed before the Ga-GaP solution comes into contact with the seed. At 1140°C, 11.36 mg was removed from a 0.235 cm^2 seed - one third of the thickness and 500 times as much as would be expected from the evaporation of the seed. When the seed was repolished and tested at 1050°C, only 0.97 mg was removed.

Thus a run was carried out using 1050°C as an operating temperature. A fresh source was used: 5.0 g Ga, 0.50 g GaP, 4.0 mg Zn. At 1050°C, 5.0 g Ga will be saturated by 0.30 g GaP. This GaP source material was Asarco semiconductor grade, prepared in silica. The furnace was heated to 1050°C, then turned off and tilted. The maximum temperature reached was 1055°C; then the initial cooling rate was about 11.5°C/min. The resulting layer was about 44 μ thick, 30 μ of seed having been removed before the layer grew. There was still evidence of a surface layer, although in this run it was only 6 μ thick.

Future work will be directed toward obtaining a planar p-n junction with minimum removal of the seed surface. Crystal perfection and doping of the overgrowth layer will be studied.

REFERENCES

1. L. L. Chang, Sol. State Electron., 7, 853 (1964).

2. C. H. Ting, private communication.

3. H. J. Queisser, J. Electrochem. Soc., 110, 52 (1963).

4. F. V. Williams, Trans. AIME, 239, 703 (1967).

5. G. S. Kulikov and E. I. Givargizov, Sov. Phys.-Sol. St., 8, 2670 (1967).

6. H. Nelson, RCA Rev., 24, 603 (1963).

7. F. A. Trumbore, M. Kowalchik, and H. G. White, Journ. Appl. Phys., 38, 1987 (1967).

8. M. R. Lorenz and M. Pilkuhn, Journ. Appl. Phys., 37, 4049 (1966).

9. R. N. Hall, J. Electrochem. Soc., 110, 385 (1963).

FIGURE CAPTIONS

Fig. 1 Carrier concentration vs. mobility for 42 GaP crystals grown between 1-1-65 and 6-1-67.

Fig. 2 Junction depth and spike depth vs. 1/T normalized to one hour.

Fig. 3 Liquid epitaxial overgrowth LEP1 cross section (cleavage face) etched in {111}Ga etchant.

Fig. 4 Liquid epitaxial overgrowth LEP1 growth surface, (111)P.

Fig. 5 Liquid epitaxial overgrowth LEP1 cross section on $(\bar{1}\bar{1}\bar{1})$Ga plane etched in {111}Ga etchant. Roughness of surfaces is due to sectioning technique.

Temp.	Time	Junction Depth	Maximum Spike Depth	Junction Depth (one hour)	Effective Time	Max. Spike Depth(effective time normalized to one hour
715°C	47.66 hr	29.5 μ	165 μ	4.30 μ	47.66 hr	24.0 μ
761	11.88 hr	28.5	133	8.28 μ	11.88 hr	38.6
813	3.28 hr	29	97.5	16.0	3.28 hr	53.9
907	18.5 min	24	41	43.3	16.4 min	78.3
998	4.25 min	15	24	56.2	1.09 min	176

TABLE 1: DIFFUSION SUMMARY

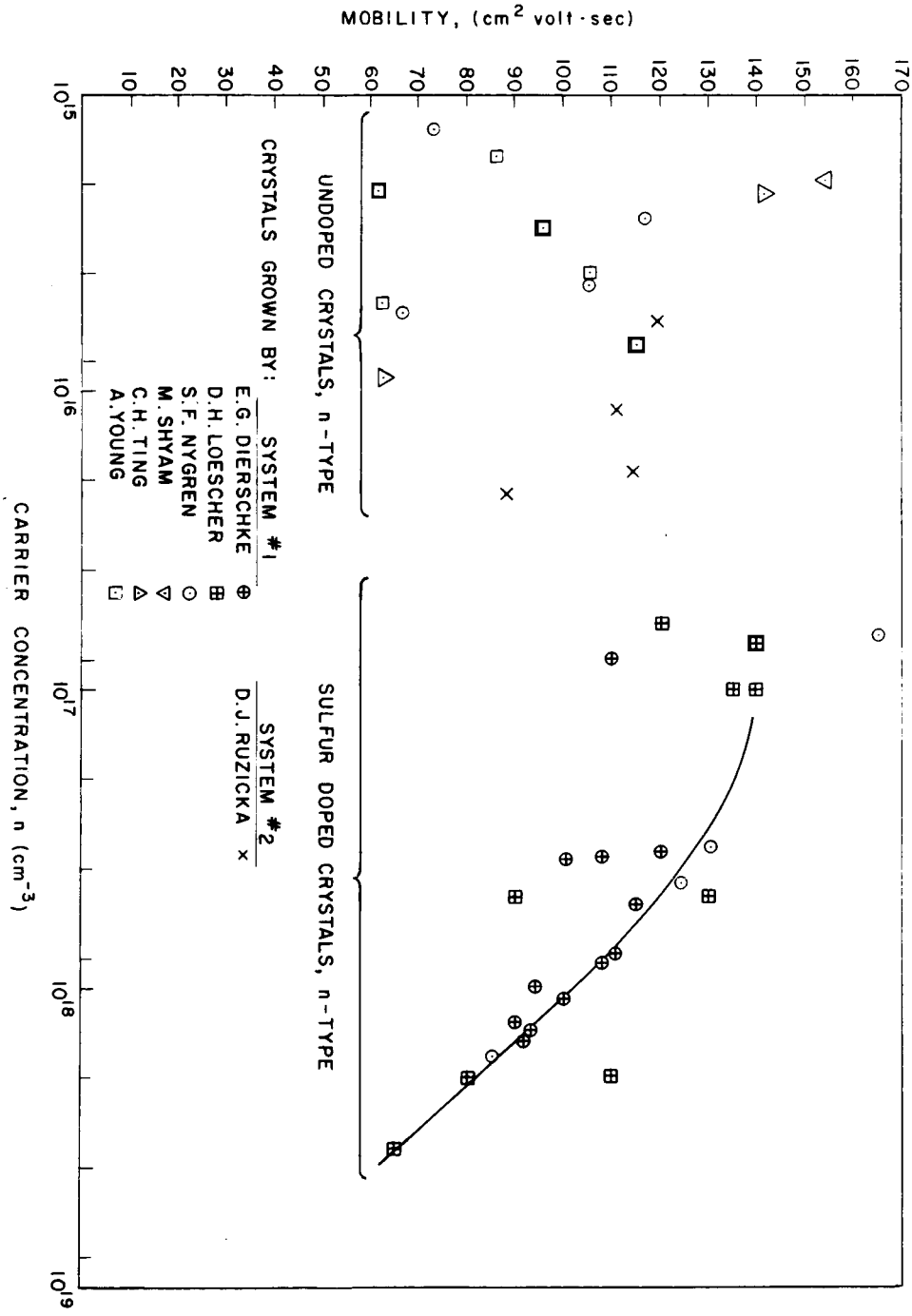
MOBILITY, (cm² volt·sec)
170
160
150
140
130
120
110
100
90
80
70
60
50
40
30
20
10
UNDOPED CRYSTALS, n-TYPE
SULFUR DOPED CRYSTALS, n-TYPE
CRYSTALS GROWN BY: SYSTEM #1
E.G. DIERSCHKE ⊕
D.H. LOESCHER ⊞
S.F. NYGREN ⊙
M. SHYAM ▽
C.H. TING △
A. YOUNG ⊡
SYSTEM #2
D.J. RUZICKA ×
10¹⁵
10¹⁶
10¹⁷
10¹⁸
10¹⁹
CARRIER CONCENTRATION, n (cm⁻³)

Fig. 1

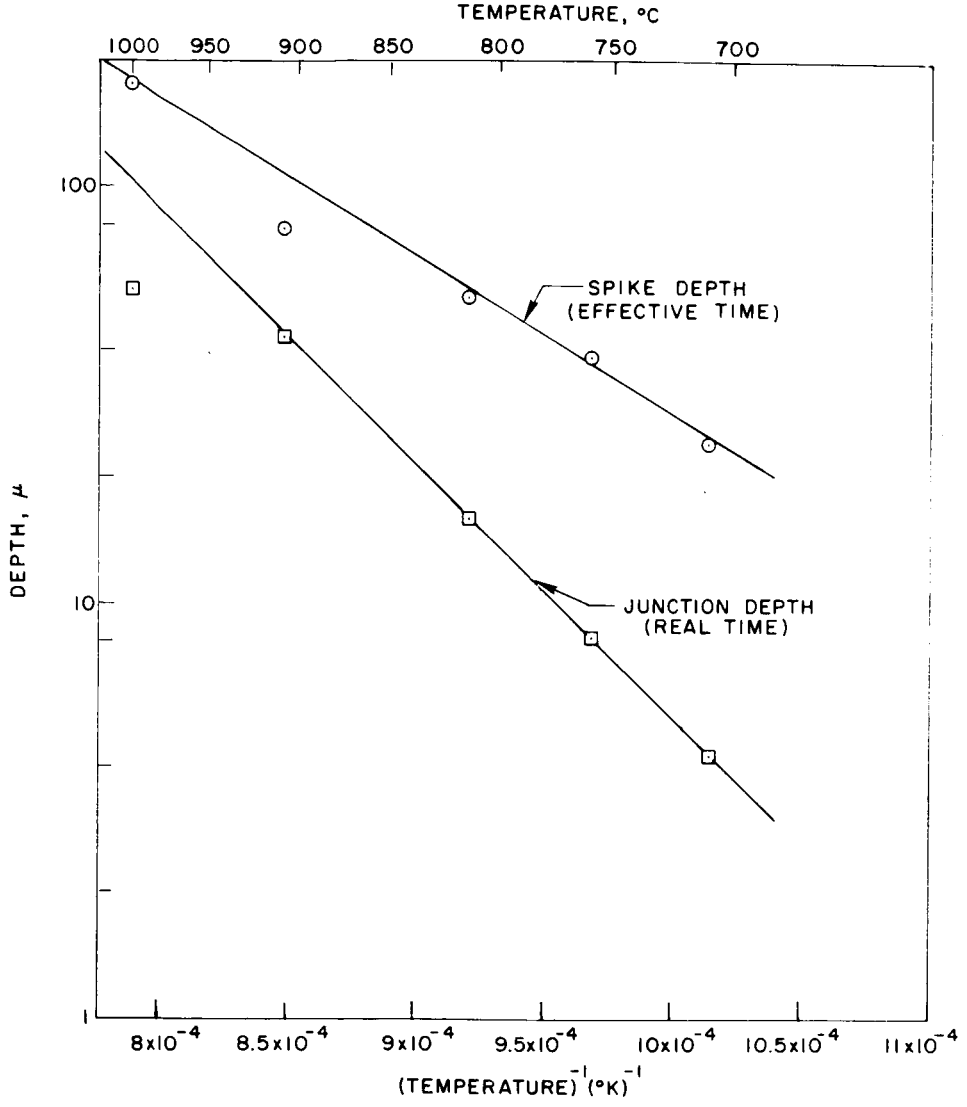
TEMPERATURE, °C
1000
950
900
850
800
750
700
100
10
1
DEPTH, μ
SPIKE DEPTH
(EFFECTIVE TIME)
JUNCTION DEPTH
(REAL TIME)
8x10⁻⁴
8.5x10⁻⁴
9x10⁻⁴
9.5x10⁻⁴
10x10⁻⁴
10.5x10⁻⁴
11x10⁻⁴
(TEMPERATURE)⁻¹ (°K)⁻¹

Fig. 2

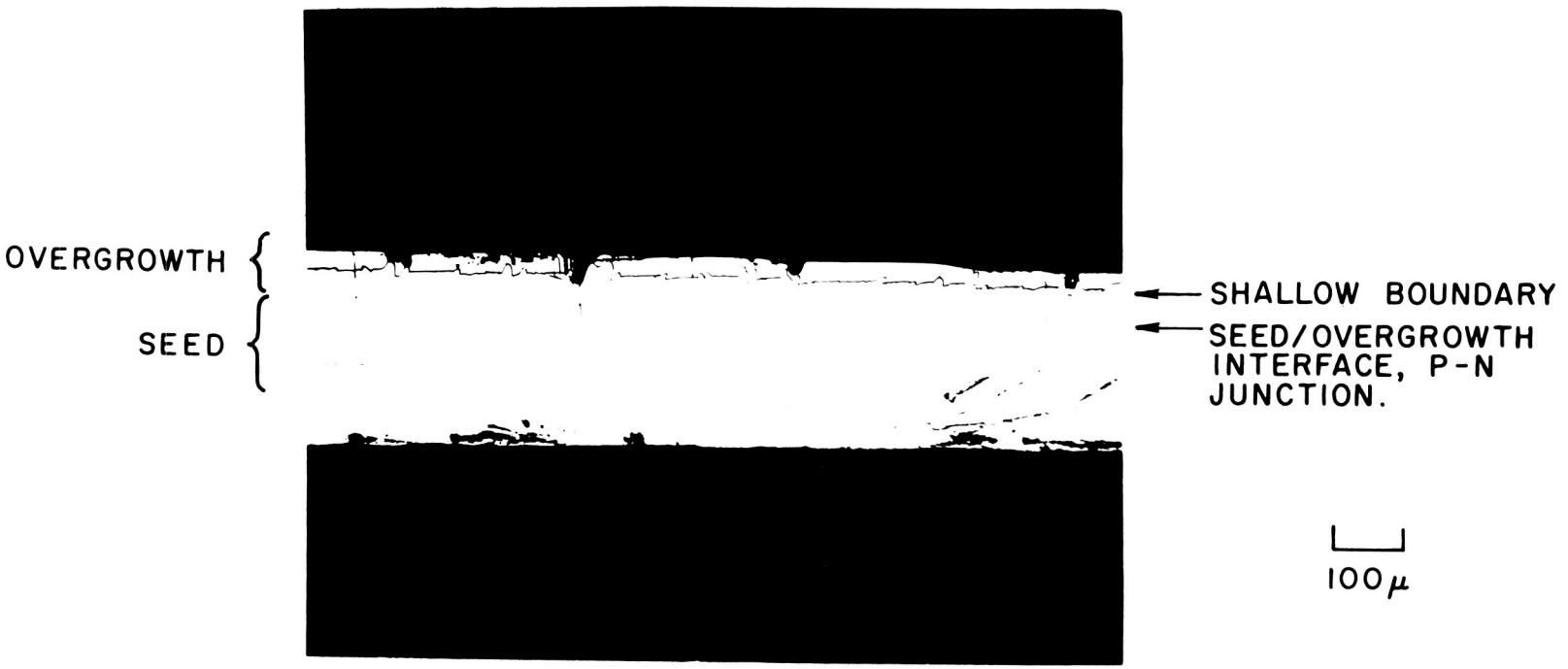
OVERGROWTH
SEED
SHALLOW BOUNDARY
SEED/OVERGROWTH INTERFACE, P-N JUNCTION.
100μ

Fig. 3

Fig. 4

Fig. 5

4) In addition, the masking effect of an evaporated SiO_2 film against sulfur diffusion, and the time variation of sulfur diffusion in GaP were briefly investigated. The results will not be discussed in this report, however, since results were not conclusive.

Results

One important modification in experimental technique was the use of a quartz plate "sandwich" to protect the surface of the samples during diffusion.[1] As discussed in the last quarterly report, this technique, while it enables better surfaces to be retained, is expected to affect the diffusion somewhat and cause uncertainties in the boundary conditions.

For the purpose of this report, however, this effect will be neglected. It would obviously be of great value to compare the results of experiments done with and without the use of the quartz plates. However, experimental conditions make it difficult to obtain reliable results when the plates are not used.

With these considerations in mind, the following results were obtained:

1. Effect of Varying Temperature - The important diffusion parameters and the corresponding diffusion profiles for temperatures $1000^{\circ}C$ - $1200^{\circ}C$ are given in Table I and Fig. 1 respectively. The major variation is due to temperature. (This may not be quite true. There is a 4:1 variation in P_2 which would cause a variation of 2 in the diffusion coefficient assuming a simple vacancy model.) The 24 hour diffusion

at 1000°C has been scaled to facilitate comparisons with the 12 hour diffusions assuming the profile is a function of $\lambda = \frac{x}{\sqrt{t}}$.

The major conclusions to be drawn from this experiment are:

a) The profiles at 1111°C and 1216°C do not appear to fit the complementary error function variation. An exponential variation gives a better fit.

b) The surface concentration at 1111°C is very high - 1.5×10^{21} cm^{-3}, approximately 6% of the phosphorus atoms in the crystal.

c) The surface concentration at 1111°C is higher than at either 1019°C or 1216°C.

d) The diffusion coefficients are very low ranging between 10^{-13} cm^2/sec and 10^{-11} cm^2/sec in the temperature range studied.

Approximate diffusion coefficients were calculated using an analytic Boltzmann-Matano method.[2] The assumptions involved in this method have not been adequately confirmed so the numbers obtained should be viewed critically. At 1111°C and 1216°C, the exponential diffusion profiles imply a concentration-dependent diffusion coefficient - in this case, in the range from 5×10^{18} to 5×10^{20} $atoms/cm^3$

$$D \propto C^{-1/3}$$

where D = diffusion coefficient and C = sulfur concentration.

A plot of D vs. 1/T for a sulfur concentration of 10^{19} cm^{-3} is shown in Fig. 2. The uncertainty in activation energy is large - it may be estimated anywhere from 1.7 to 3.3 eV. More data is needed to obtain a more accurate value.

The radiograph of the sample diffused at 1019°C reveals some localization of activity. This would tend to make the apparent diffusion coefficient larger than its true value.

The diffusion profiles shown in Fig. 1 were obtained from the better side of each diffused sample - in general these were smoother, shinier, and had a lower total integrated concentration. This is believed to be the "B" (phosphorus) face.

Occasionally the second face ("A") was also lapped. In general the values of surface concentration and diffusion coefficient were within a factor of two (usually larger) for samples diffused at 1100°C and 1200°C.

However, in the diffusion at 1019°C a very marked difference was observed in both surface concentration and diffusion coefficient. The profiles for the two faces are shown in Fig. 3. The surface concentration on the dull face was an order of magnitude larger; the diffusion coefficient on this face was six times larger and may have been even more than this (recall that it is believed that the diffusion coefficient for the shiny face is probably too large).

The sample diffused at 1019°C for 24 hours retained a highly polished surface on one side. Except for a few "canal-like" features which may have developed from polishing scratches, the surface was almost as good as the surface before diffusion.

2. Effect of Varying Sulfur Pressure - Diffusions were done at 1108°C with a fixed phosphorus pressure and sulfur vapor densities ranging from 2 - 52 micrograms/cm^3. The important parameters

of several selected profiles are given in Table II and the profiles themselves in Fig. 4 (the profiles are from the "A" face).

The major conclusion to be drawn is that the surface concentration increases as the sulfur vapor density increases. Most of the diffusions done this quarter were at 1115°C (± 5°C). Due to experimental difficulties, e.g. wedging during the lapping, most of the profiles have been discarded for the calculation of diffusion coefficients. However, a reasonable extrapolation of surface concentration is still possible and this data is shown in Fig. 5. (Data from both A and B faces is shown.) The scatter in values is again large but a reasonable fit shows that surface concentration is proportional to the sulfur pressure (vapor density) during diffusion.

This is <u>not</u> the result expected for a simple vacancy diffusion. Using a simple mass action model for the incorporation of sulfur or phosphorus sites, we can obtain

$$\frac{1}{2} S_2 \text{ (vapor)} + V_p \overset{K_1}{\rightleftarrows} S_p^o \overset{K_2}{\rightleftarrows} S_p^- + n$$

$$[S_p^o] = K_1 [V_p] (P_{s2})^{1/2}$$

$$[S_p^-] = K_2[S_p^o]/n = K_1K_2[V_p](P_{s2})^{1/2}/n$$

where

V_p = phosphorus vacancy

S_p^o = neutral sulfur atom on phosphorus site

S_p^- = ionized sulfur atom

n = electron concentration

K_1, K_2 = equilibrium constants.

For the case where most of the sulfur is ionized and the semiconductor is extrinsic, i.e. $[S_p^-] = n$.

$$[\text{Total sulfur}] \approx [S_p^-] \alpha (P_{s2})^{1/4} \quad .$$

For the case where most of the sulfur is neutral

$$[\text{Total sulfur}] \approx [S_p^o] \alpha (P_{s2})^{1/2}$$

These two cases do not fit the observed experimental results, where

$$[\text{Total sulfur}] \alpha \ P_{s2}$$

Our results do not agree with reported data for the solubility of sulfur in GaP at 1040°C as a function of the melt composition.[3] Some agreement with a simple vacancy model was obtained in Trumbore's experiments.

The great difference in the shape of the profiles is not understood. At low surface concentrations, the profile appears to fit the complementary error function solution. However, only four data points are obtained and this conclusion is not necessarily valid.

A distinct difference in the shapes of profiles would imply that the diffusion constant was not only a function of sulfur concentration. In this case application of the Boltzmann-Matano method would not be meaningful.

In one instance, where an unusually large penetration depth was obtained, the result was attributed to the surface roughness of the sample. This is not believed to be the case for diffusion AL-6.

Goldstein has reported a profile with an initial flat region for the diffusion of Se in GaAs. This was attributed to the formation of a selenium glass on the GaAs surface. A check for a similar substance in our experiment will be performed next quarter. However, x-ray diffraction on this sample thus far has failed to reveal the presence of any other phase besides GaP.

3. Effect of Varying Phosphorus Pressure

This experiment is potentially the most powerful for determining the diffusion mechanism. By changing the phosphorus pressure over the sample during diffusion, the stoichiometric balance of gallium and phosphorus vacancies may be changed. The variation of diffusion coefficient with phosphorus pressure can reveal which vacancies are involved in the diffusion process. (Schottky, however, has stated that the crystal may not be in equilibrium with the vapor.[5] Dislocations will try to maintain a stoichiometric balance in the crystal. Equilibrium with the vapor must take place by vacancy diffusion from the surface which is a much slower process. Thus a pre-diffusion anneal under diffusion conditions may be necessary.)

Diffusions were done at 1115°C under 0.6 ATM (P_2) and also with no excess phosphorus. Unfortunately, decreasing the phosphorus pressure also increases the rate of surface deterioration. In the experiment performed under these conditions, the equivalent of 8 microns was lost from each face so results are not reliable. However, the change in diffusion coefficient does not appear to be anywhere near as much as would be expected for a simple vacancy diffusion

mechanism. Further work will be necessary on this most important experiment. Prediffusion anneals may be necessary and intermediate pressures (P_2) should be used.

Discussion

The data presented in this quarterly report is believed to be the most reliable of the work done to date. Surface quality, weight loss, autoradiographs, and the quality of the lapping procedure are the principal criteria used in judging the merits of the data obtained.

However, many qualifying statements should be made:

1) The reproducibility of results has not been adequately checked. In the one instance where four diffusions were done under virtually the same conditions, surface concentrations and diffusion coefficients were found to vary by a factor of five. (This may be an extreme case since the profiles were shallow and contained only 4 - 5 points.) Although the scatter is large, the data is still adequate for illustrating trends. However, the weakness in relying too heavily on a single experimental point should be stressed.

2) The possible dependence of diffusion on the material used has not been studied. It is known that the diffusion of zinc in the epitaxial GaP grown at this laboratory depends markedly on the presence of certain crystal defects (possibly stacking faults). Whether sulfur diffusion behaves similarly is not yet known.

3) The data is often inconsistent. For example, the diffusion coefficient calculated from different profiles for fixed temperature and phosphorus pressure would suggest that the diffusion

coefficient is not simply a function of sulfur concentration. The applicability of the Boltzmann-Matano method would seem questionable if this were the case. The issue is made more complex by the use of the quartz plates and the fact that the sulfur source is usually significantly depleted during diffusion.

4) Various researchers working with sulfur in GaAs have reported difficulties with surface erosion attributed to compound formation. X-ray diffraction on several samples has failed to reveal conclusive evidence of any phase besides GaP. The nature of the difference between profiles on "A" and "B" faces must be studied further.

Plans for Next Quarter

During the next quarter we hope to resolve some of these problems. Further experiments to check reproducibility will be done. Dependence of the surface concentration on sulfur vapor density for higher temperatures (1200°C) will be of interest. Since sulfur incorporation in GaAs and GaP has often been interpreted in terms of a sulfur-vacancy complex[6] (essentially a solid solution between GaP and the Ga_2S_3 compound) significant differences may be expected for temperatures above and below the melting point of the compound. (T_{melt} for Ga_2S_3 is now believed to be 1090°C[7]. However, this figure may be subject to revision.)

We hope to study the electrical properties of the diffused layer. Also p-n junctions will be made to study the geometrical configuration of the diffusion front (whether planar, with spikes, etc.).

To study the dependence of diffusion on phosphorus pressure, time, and temperature we plan to use a Ga_2S_3 diffusion source and

p-n junction staining. This will necessitate the growth of lightly-doped p-type material. However, several advantages may be realized:

1) For the lower surface concentrations expected from the compound source, better surfaces (without the use of quartz plates) should be possible.

2) An infinite source condition can be maintained.

3) Experimental procedure will be easier than determination of diffusion profiles. However, an erfc variation may have to be assumed.

4) Interpretation of the data should be easier assuming a negligible out diffusion of the p-type dopant.

REFERENCES

1. R. W. Fane and A. J. Goss, Solid-State Elec., 6, 383 (1963).
2. L. D. Hall, J. Chem. Phys., 21, 87 (1953).
3. F. A. Trumbore et al, J. Electrochem. Soc., 112, 782 (1965).
4. B. Goldstein, Phys. Rev., 121, 1305 (1961).
5. G. Schottky, J. Phys. Chem. Solids, 27, 1721 (1966).
6. L. J. Vieland and I. Kudman, J. Phys. Chem. Solids, 24, 437 (1963).
7. R. M. A. Lieth et al, J. Electrochem. Soc., 113, 789 (1966).
8. C. D. Thurmond, J. Phys. Chem. Solids, 26, 785 (1965).

FIGURE CAPTIONS

Fig. 1 Diffusion profiles of sulfur in GaP (effect of varying temperature)

Fig. 2 Variation of diffusion coefficient with temperature.

Fig. 3 Diffusion profiles of sulfur in GaP (diffusion at 1019°C - comparison of A and B faces).

Fig. 4 Diffusion profiles at sulfur in GaP (effect of varying sulfur pressure).

Fig. 5 Dependence of surface concentration on sulfur pressure ($T = 1115^{\circ}C$).

Diffusion	C-2	B-2a	C-1
Temperature ($^{\circ}C$)	1018	1111	1215
Sulfur Density (micrograms/ml)	18.5	18.0	20.5
Phosphorus Density (milligrams/ml)	2.2	2.0	2.1
Phosphorus Pressure (P_2-atm)	0.31	0.6	1.1
Time (hours)	24	12	12

TABLE 1 - Diffusion Parameters

Diffusion	AL-9	B-2b	AL-6
Temperature ($^{\circ}C$)	1106	1111	1110
Sulfur Density (micrograms/ml)	2.09	18.2	51.5
Phosphorus Density (milligrams/ml)	1.64	1.96	1.73
Time (hours)	12	12	12

TABLE II - Diffusion Parameters

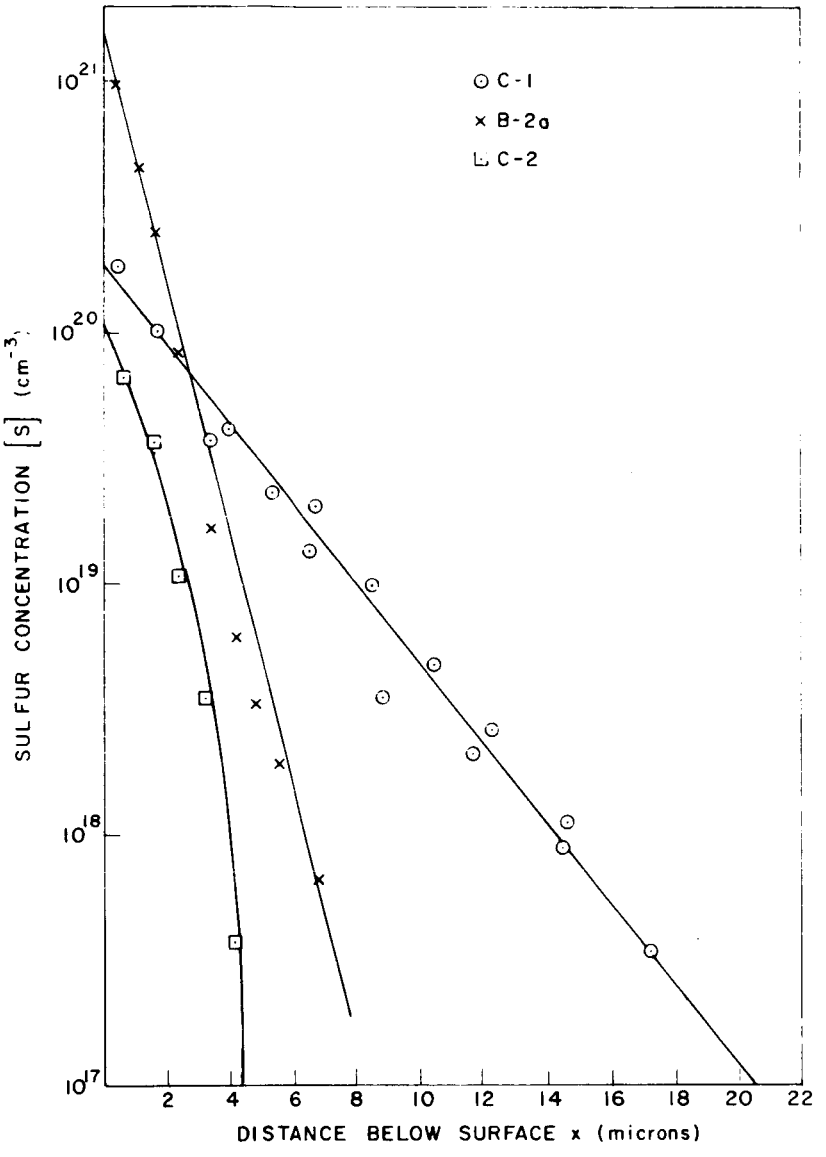
⊙ C-1
× B-2a
□ C-2
10^{21}
10^{20}
10^{19}
10^{18}
10^{17}
SULFUR CONCENTRATION [S] (cm^{-3})
2
4
6
8
10
12
14
16
18
20
22
DISTANCE BELOW SURFACE x (microns)

Fig. 1

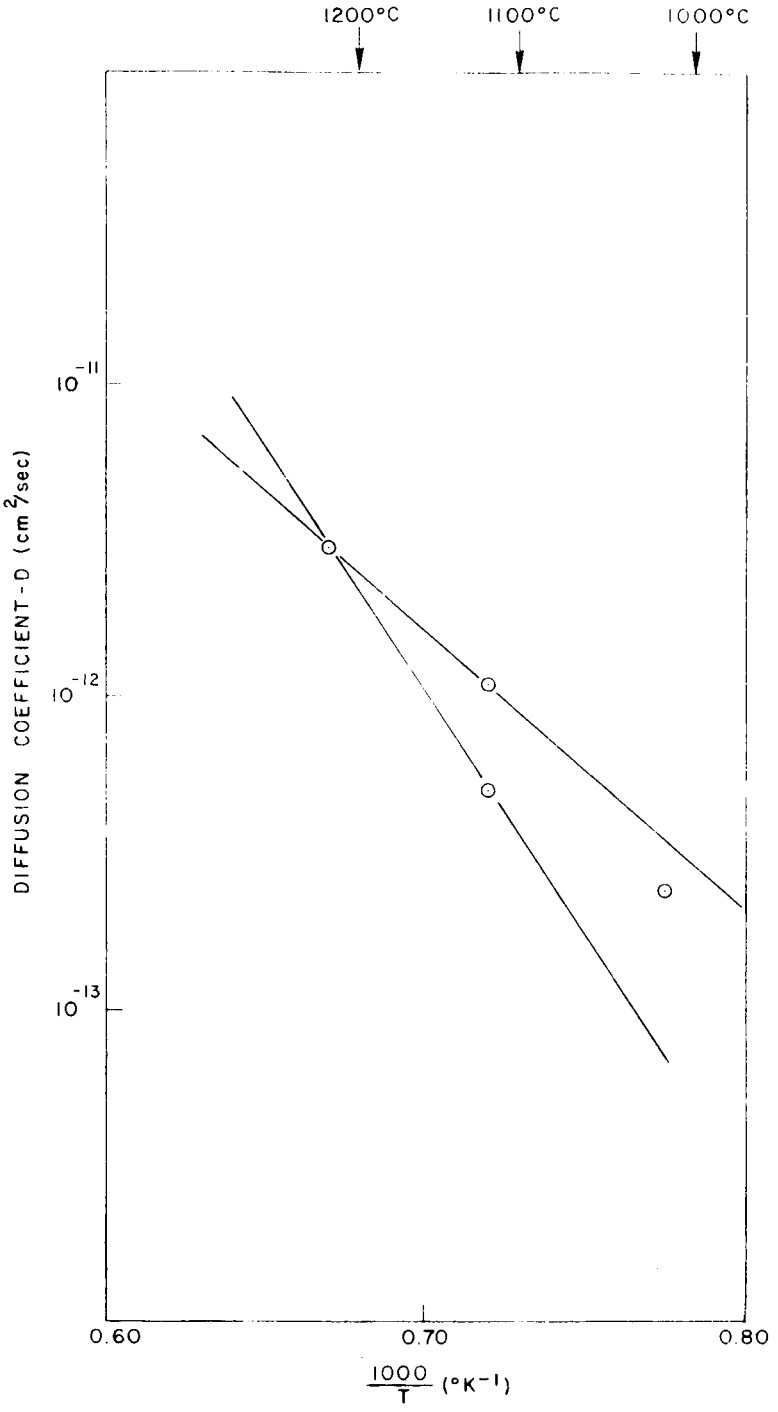
1200°C
1100°C
1000°C
DIFFUSION COEFFICIENT - D (cm²/sec)
10⁻¹¹
10⁻¹²
10⁻¹³
0.60
0.70
0.80
1000/T (°K⁻¹)

Fig. 2

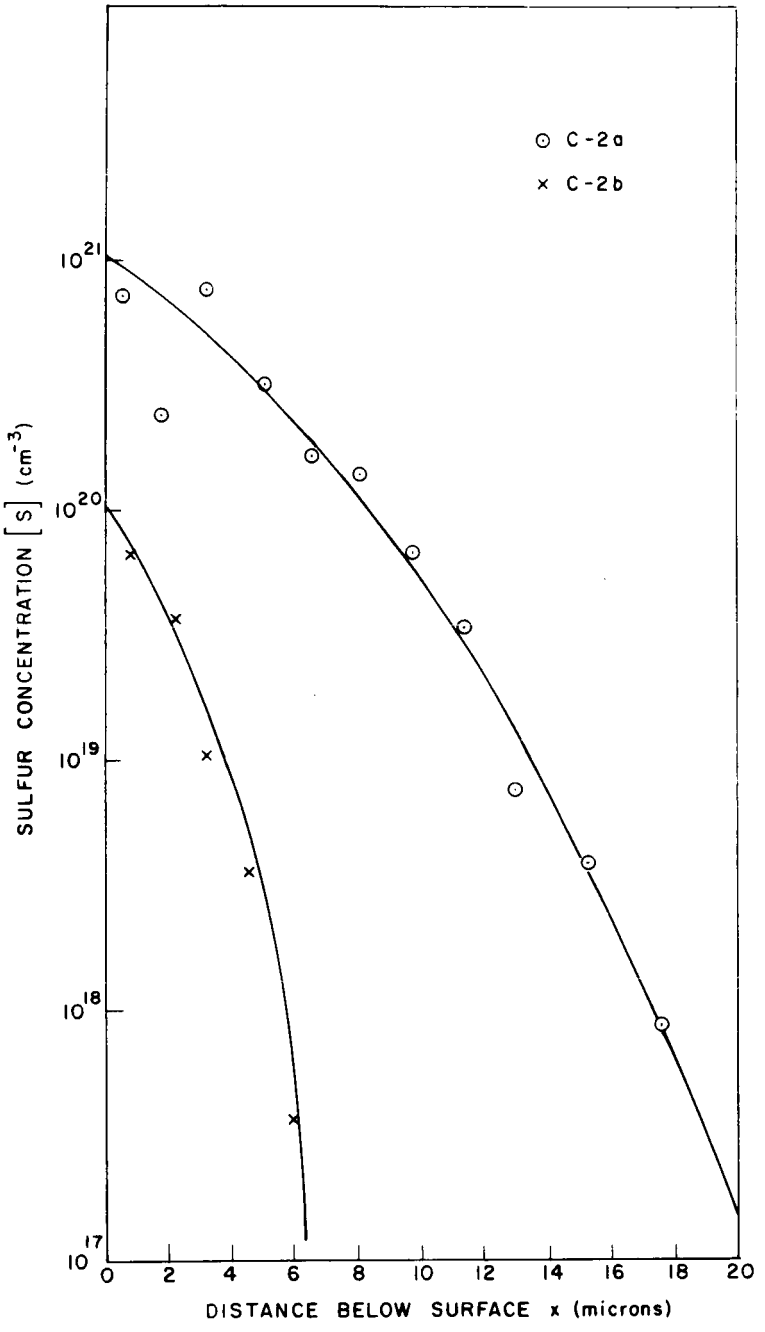
⊙ C-2a
× C-2b
SULFUR CONCENTRATION [S] (cm⁻³)
10²¹
10²⁰
10¹⁹
10¹⁸
10¹⁷
0
2
4
6
8
10
12
14
16
18
20
DISTANCE BELOW SURFACE x (microns)

Fig. 3

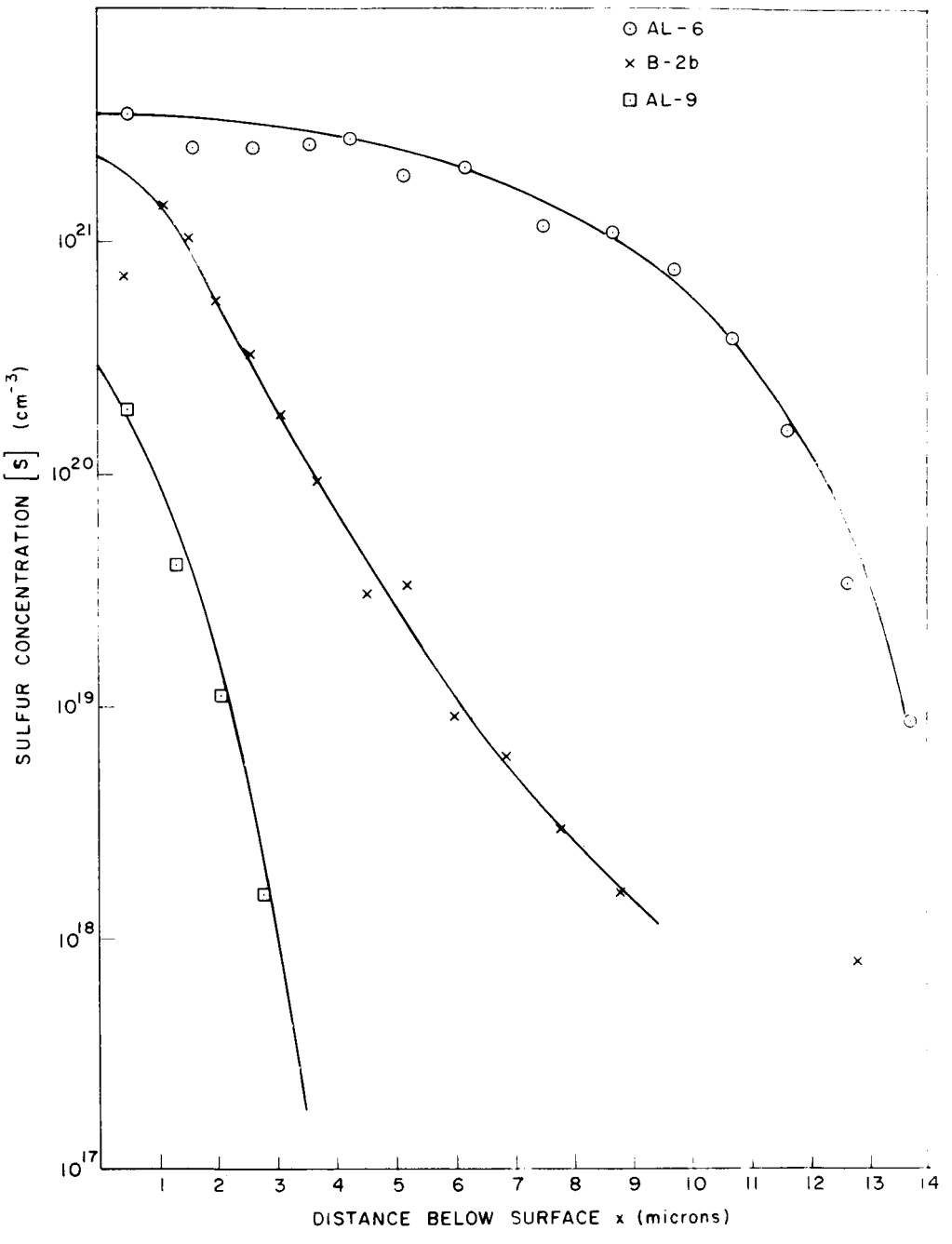
⊙ AL-6
× B-2b
⊡ AL-9
SULFUR CONCENTRATION [S] (cm⁻³)
10²¹
10²⁰
10¹⁹
10¹⁸
10¹⁷
1
2
3
4
5
6
7
8
9
10
11
12
13
14
DISTANCE BELOW SURFACE x (microns)

Fig. 4

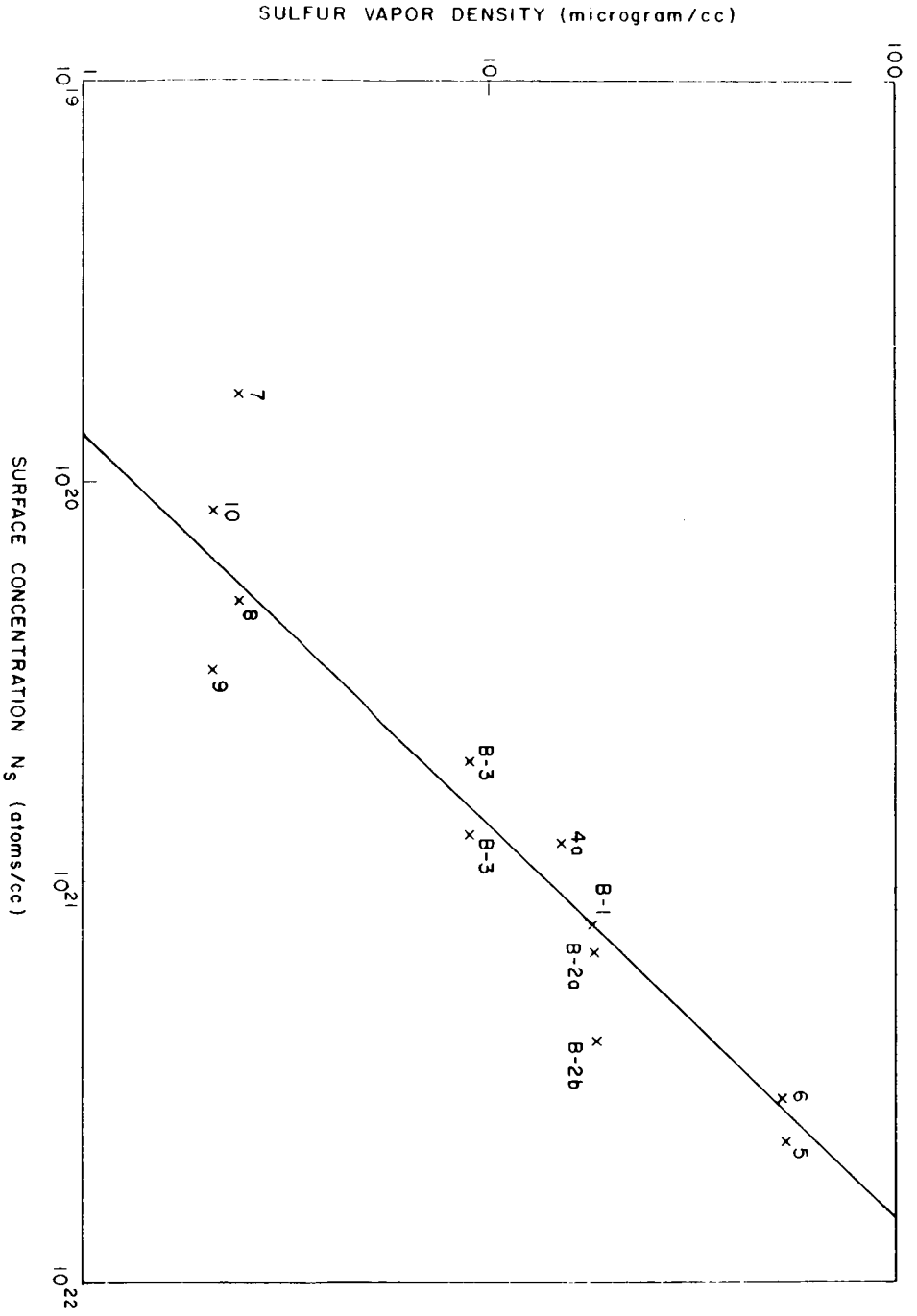
SULFUR VAPOR DENSITY (microgram/cc)
1
10
100
10^{19}
10^{20}
10^{21}
10^{22}
SURFACE CONCENTRATION N_S (atoms/cc)
7
10
8
9
B-3
B-3
4a
B-1
B-2a
B-2b
6
5

Fig. 5